Optogenetic Modulation of Corticostriatal Activity for the Regulation of Social Dominance

Modelação optogenética de actividade cortico-estriatal na manipulação de dominância social

Dissertação de mestrado em Biologia Celular e Molecular, com especialização em Neurobiologia, orientada pelo Doutor João Peça e supervisionada pela Professora Ana Luísa Carvalho, apresentada ao Departamento de Ciências da Vida da Faculdade de Ciências e Tecnologia da Universidade de Coimbra
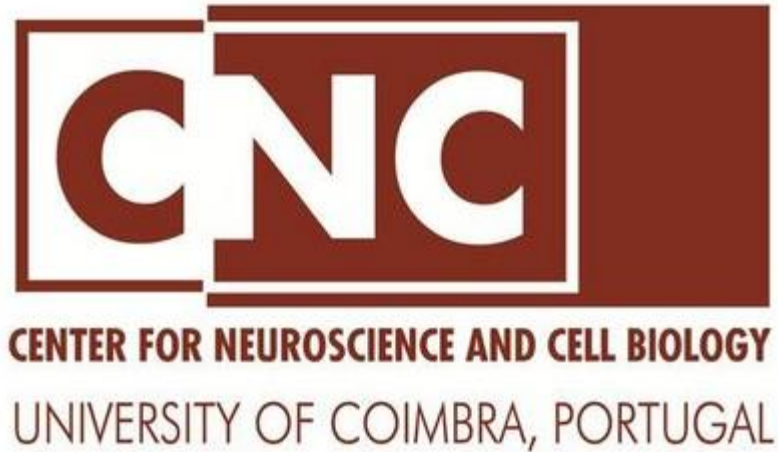
José Pedro Pinto Sampaio

Coimbra, 2018

· U C ·

UNIVERSIDADE DE COIMBRA

This work was developed at the following institution:

At the **Neuronal Circuits and Behavior Group** - Center for Neurosciences and Cell Biology, University of Coimbra

Acknowledgments

Table of Contents

List of Abbreviations

ac; aca - anterior commissure

AC; AAC – anterior cingulate cortex

AAV – adeno-associated virus

AcbC – nucleus accumbens core

AcbSh – nucleus accumbens shell

ACd - dorsal anterior cingulate cortex

aCSF – artificial cerebral spinal fluid

Aid - dorsal agranular insular cortex

Aiv - ventral agranular insular cortex

ANOVA – analysis of variance

AOM – anterior olfactory nucleus, medial region

AOP – anterior olfactory nucleus, posterior region

Arc - activity-regulated cytoskeleton-associated protein

ATP-Mg - adenosine 5'-(tetrahydrogen triphosphate) magnesium salt

BLA – basolateral amygdaloid nucleus, anterior part

BLP – basolateral amygdaloid nucleus, posterior part

CA1 – field CA1 of hippocampus

CA2 – field CA2 of hippocampus

ChR2 – channelrhodopsin-2

Cl - claustrum;

CM - central medial thalamic nucleus

CPu - caudate putamen

CsCl - cesium chloride

CsMeSO$_3$ - cesium methanesulfonate

CTB – cholera toxin, sub-unit b

DAPI - 4',6-diamidino-2-phenylindole

IX

D-APV - (2*R*)-amino-5-phosphonovaleric acid

DEn - dorsal endopiriform nucleus

DLPFC - dorsolateral prefrontal cortex

dmPFC – dorsomedial prefrontal cortex

DOM - dominant

DV – dorso-ventral

EGTA - ethylene glycol-bis(β-aminoethyl ether)-N,N,N',N'-tetraacetic acid

EYFP – enhanced yellow fluorescence protein

fmi - forceps minor of the corpus callosum

fMRI - functional Magnetic Resonance Imaging

fr - fasciculus retroflexus

GTP-Na - Guanosine 5'-triphosphate sodium

GC – genome copy

Hcl - hydrochloric acid

HEPES - 4-(2-hydroxyethyl)-1-piperazineethanesulfonic acid

hSyn – human synapsin gene promoter

IEG – immediate early gene

IL – infra-limbic cortex

IP – intra-peritoneally

IPS - intraparietal sulcus region

mEPSC – mini excitatory post-synaptic current

ML – medio-lateral

mM - milimolar

MOhm - megaohm

MSN – medium spiny neuron

mW - miliWatt

MW – molecular weight

NA – numerical apperture

NAcc - nucleus accumbens

NaCl – sodium chloride

NMDG - N-Methyl-D-glucamine

PBS – phosphate-buffered saline

PFA - paraformaldehyde

PFC - prefrontal cortex

Pir – piriform cortex

PLd - dorsal prelimbic cortex

PLv - ventral prelimbic cortex

PrL; PL – pre-limbic cortex

PT - paratenial thalamic nucleus

PV – paraventricular thalamic nucleus

PVA – paraventricular thalamic nucleus, anterior part

rACCg - rostral anterior cingulate gyrus

RC – rostro-caudal

rmPFC - rostromedial prefrontal cortex

sEPSC – spontaneous excitatory post-synaptic current

SC – sub-cutaneous

STS - superior temporal sulcus region

sm – stria medullaris of the thalamus

SMA - supplementary motor area

Str - striatum

SUB - subordinate

TEA-Cl - tetraethylammonium chloride

Thal - thalamus

TPJ - temporo-parietal junction

TTX - tetrodotoxin

VLPFC - ventrolateral prefrontal cortex

vmPFC - ventromedial prefrontal cortex

Abstract

Social hierarchies can be understood as a form of dominance, essential for animal species that live under communal systems, allowing the allocation of resources and assignment of responsibilities according to skill set, while also increasing social motivation and maximizing the group's survival odds. Studying social hierarchies in a laboratory setting normally resorts to rodents, which naturally possess a distinct set of dominance behaviors. Laboratory mice, grown and cohabiting within the constraints of their home-cages, establish a social hierarchy according to a dominance rank. The tube test paradigm, where mice are paired in a round-robin manner to induce non-aggressive disputes of social dominance, is particularly accurate in reflecting dominance rank and strongly correlates with other social dominance behaviors.

As we gain more knowledge on the neural mechanisms behind the regulation social hierarchy behaviors, the pre-frontal cortex (PFC) is proposed as a major player in the processing of most relevant information and exerting top-down control over behavior. Another brain region of interest is the ventral striatum, which has also been described as being involved in social hierarchy processing and in the motivational and effort-based aspects of behavior. Importantly, cortical projections between the mPFC (medial pre-frontal cortex) and Nucleus Accumbens (NAcc; belonging to the ventral striatum) have been widely described to guide murine behavior during non-social and, more recently, during social contexts as well.

Optogenetics may enable the modulation of this neural circuit and help elucidate the function of the cortical projections between the mPFC and NAcc.

Keywords: social hierarchy, dominance, medial prefrontal cortex (mPFC), nucleus accumbens (NAcc), mPFC-NAcc projections, optogenetics

Resumo

A formação de uma hierarquia social pode ser vista como uma manifestação de dominância e é essencial para o correcto funcionamento de espécies animais que vivem em comunidade. Permitem alocar recursos e distribuir responsabilidades entre os elementos constituintes de forma eficaz, aumentar os indices de motivação e maximizar a probabilidade de sobrevivência. O estudo deste fenómeno é feito, por norma, usando espécies roedoras, que manifestam um distinto leque de comportamentos de dominância social na Natureza. Ratinhos de laboratório são mantidos em gaiolas, onde crescem e cohabitam em espaço partilhado, formando uma hierarquia social estável desde cedo. O designado "Tube Test", que consiste em colocar dois indivíduos em cada uma das pontas de um tubo apertado, de modo a induzir disputas não agressivas, revela-se bastante eficaz no evidenciar de relações de dominância entre um determinado grupo de ratinhos de laboratório.

Estudos sobre os mecanismos neuronais por detrás das hierarquias sociais implicaram o cortéx pré-frontal medial (mPFC) como principal centro cerebral responsável pelo processamento de informação e manifestação comportamental. Outra região, o estriado ventral, está também descrito como reunindo funções no processamento de hierarquias sociais, assim como em aspetos comportamentais ligados à motivação e esforço. Estas duas regiões connectam via projeções neuronais que ligam o mPFC ao *nucleus accumbens* (NAcc), que se encontra na região mais ventral do estriado. Também já se encontra descrito que estas projeções determinam o comportamento de ratinhos, tanto em contextos não-sociais como sociais.

A optogenética é uma técnica que possibilita a modelação da actividade de circuitos neuronais, podendo ajudar a elucidar o papel das projeções corticais que ligam o mPFC ao Nacc.

Palavras-chave: hierarquia social, dominância, cortéx pré-frontal (mPFC), nucleus accumbens (Nacc), projeções mPFC-Nacc, optogenética

Chapter 1 | Introduction

1.1 - Social Hierarchy

The concept of hierarchical stratification and its impact on social organization dates back to the 1920s, when Schjelderup-Ebbe described the innate ability of domestic fowls to arrange into a structured hierarchy by order of individual dominance[1].

Hierarchization in social groups can be understood as a form of dominance expression, essential for animal species that live under communal systems. Moreover, it is widely accepted that social stratification influences health and behavior, mostly in males, for whom higher social positions usually imply facilitated access to food, resting spots and mate partners[2]. Social rank can also reflect on an individual's physical appearance, as it happens with the dominant males in orangutan societies who develop large flappy cheek-pads[3,4]. Fish, mammals and most every other vertebrate species that live in a social context have also adopted and evolved social hierarchies where males at the top of the rank enjoy several perks[5].

On the other hand, studies have also shown that maintaining a high social rank can be both physically and physiologically demanding. For example, prioritized access to resources usually means greater time spent fighting, which increases dominant individuals' probability to get injured, besides being demanding energy-wise[6,7]. Nonetheless, the evidence that hierarchical organization benefits the entire group fitness can be observed by the widespread prevalence of this form of organization in nature[8]. It is thought that hierarchies assist in the efficient distributing of goods[9] and in the assignment of responsibilities among members with different skills and social rank[10], therefore enhancing the groups' survival chances as a whole.

In nature, physical dominance mostly determines social rank, however, humans societies have settled to rank individuals depending on cognitive skills, such as intelligence and emotional stability, income, skills, career success, popularity and prestige, all of which have been shown to weigh-in in human's assessment of status[11–15]. Humans are also known to defer their actions and opinions to individuals who possess particular traits of value to the community[16]. Assuming that these individuals gather ideal physical or intelligence features, following and learning from them can also be beneficial to the entire group, increasing motivation and productivity[10,17]. For these reasons, ranking humans into a social hierarchy is a complex process since it does not rely only on a single dominant or valued trait, but rather on a combination of features valued by the community[18].

1.2 - Laboratory Rodent Social Hierarchies

In a naturalistic setting, inherent social dominant behaviors of mice include: prioritized access to food and grooming, low interest for labour activities, antagonistic behaviors towards other males and pro-active establishment of territory and courtship of the females[19]. Dominant rodents are also known to display plastic social behavior[19], being more aggressive and territorial in low population density but compromising and more tolerable if living within a large group of

animals, in which case only one male asserts himself as dominant while all other become subordinates[20,21]. The same applies to laboratory mice living within their home-cages, where natural restraints lead the animals to establish a social hierarchy to avoid constant fighting[22]. In a laboratory setting, dominance can be displayed by mice through several behaviors **(Figure 1)**. Dominant males are, for example, known to barber their more submissive cage-mates, excessively plucking the whiskers and scrubbing their hair during mutual grooming, in a phenomenon known as *'Dalila effect'*[23], and to emit 70 kHz ultrasonic vocalizations during female courtship[24,25].
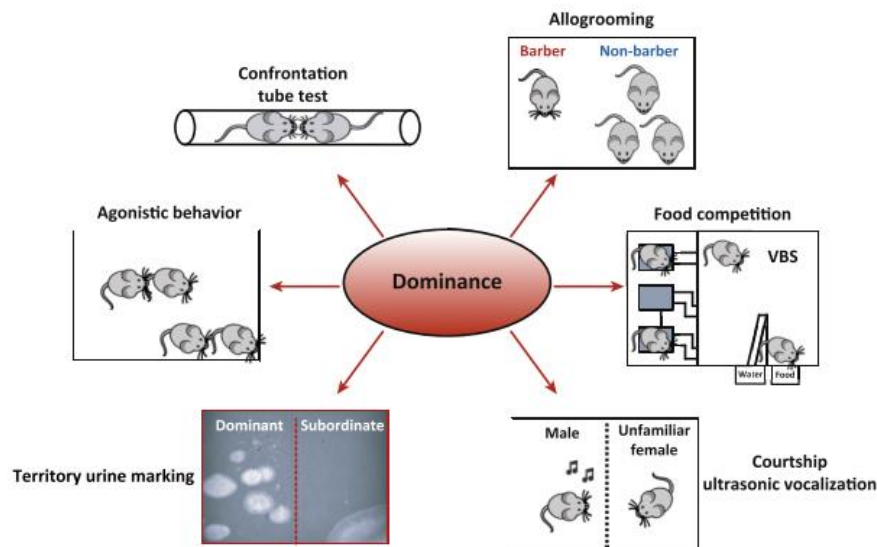
Figure 1 – Different behavioral measures of social dominance for laboratory rodents. Dominance is the common underlying factor of the several rodent behaviors depicted. *Adapted from Wang, F. et al. The mouse that roared : neural mechanisms of social hierarchy (2014).*

Importantly, each of the dominant behaviors displayed by mice in the wild can have a correspondent paradigm to help determine social rank among laboratory mice. One of these paradigms - the tube test - has been shown to be a good indicator of social dominance, with strong correlations with other dominance tests[26]. The tube test consists of placing two mice at each end of a narrow tube, forcing them to meet in the middle. The test ends in a non-violent manner, when one of the mice is forced to retreat. Since mice resist backing out towards a place they cannot see, the animal that forces the opponent to retreat is scored as the more dominant of the pair[26]. Tube test winner mice have been described to be more active during these confrontations, initiating more and longer pushes than loser mice and, conversely, offering more resistance when being pushed, with more frequent push-backs and fewer retreats[27]. By repeating this test under a round-robin arrangement, a dominance order can be determined for a laboratory mice population, ranking individuals according to how many tube test victories they scored[28,29]. The confrontation inside the tube will also take longer the closer the two mice are in rank[27].

Tube test results correlate well with many of the other aforementioned dominance test paradigms. Previous studies have reported that barbering mice are also tube test winners over their cage mates[29–31] and that top performers in the tube test are also more sensitive to female stimuli, emitting significantly more vocalizations than subordinate mice[24,29,32].

The order in which mice are submitted to the tube test and the other paradigms of social dominance does not have an impact on the final outcome[29], implying that submitting the mice to the tube test does not induce an artificial hierarchy in itself.

1.3 – Social Cognition and Social Status Perception in Animals

Living within a stratified animal society, where complex social interactions occur frequently, requires each individual to be able to express and recognize social status cues, such as visual and vocal signals, which serve to convey social rank and guarantee appropriate social behavior[9,33,34]. For example, analyzing competitor's physical cues serves as an immediate and reliable visual input about their overall strength and, possibly, motivations[35]. In time, animals learn their position in the hierarchy directly through competitive dyadic interactions but can also infer upon other's and their own relative hierarchical status from observing their behaviors and interactions within the social group[34]. This is known as "transitive inference" and implies that social information can be learned merely through observation[36].

During tube test encounters, mice are able to convey hierarchical status through facial, odor and ultrasonic cues[37,38]. During periods of investigation, dominant and subordinate individuals display very different patterns of sniffing frequency, which might also constitute an effective way to relay information about social rank[39].

1.4 - Neural Basis of Social Hierarchy Processing

As described so far, the establishment of dominance hierarchies requires a wide range of cognitive skills and capabilities, including the perception of social norms and social ranks.

Although the neural mechanisms controlling social dominance and hierarchies behaviors remain vague, in the past recent years, the use of powerful imaging techniques has given some knowledge on which brain regions are recruited during cognitive and social tasks. Based on human studies using functional Magnetic Resonance Imaging (fMRI), it is possible to attribute social status recognition to different neuronal circuits of cortical brain regions: the occipitotemporal and parietal cortices are involved in perceptual and attentional processes and help infer social status[14,40,41], whereas, processing social hierarchies is responsibility of the prefrontal cortex (PFC), the central core for executive behavioral control[42]. Indeed, studies conducted within a simulated social context revealed that distinguishing the faces of high and low-ranked players requires selective activation of the dorsolateral region of the PFC[14] (DLPFC), a brain region also involved in social skills such as interpersonal[43] and social moral judgments[44]. In turn, the ventrolateral PFC (VLPFC) responds to nonverbal cues of high social status, such as

body posture[45], whilst the medial PFC was found to be recruited to recognize the intentions and motives, but also to form judgements, of others[46] and to be evoked in an unstable hierarchy setting[14] **(Figure 2)**. Moreover, the medial PFC can be further subdivided in the rostromedial (rmPFC), dorsomedial (dmPFC) and ventromedial (vmPFC) partitions, all of them implicated in distinct human social behaviors. Indeed, fMRI studies show that vmPFC is implicated in social reward[47] and social acceptance[48] and that decreased vmPFC activity may also signify social motivation deficits[49]. Moreover, the rmPFC and dmPFC regions are usually recruited during social cognitive tasks that involve one´s own and others perception, including making judgments of mental state, with the rmPFC more involved in self-referential tasks[51,56] and the dmPFC more engaged in perception of others[55].
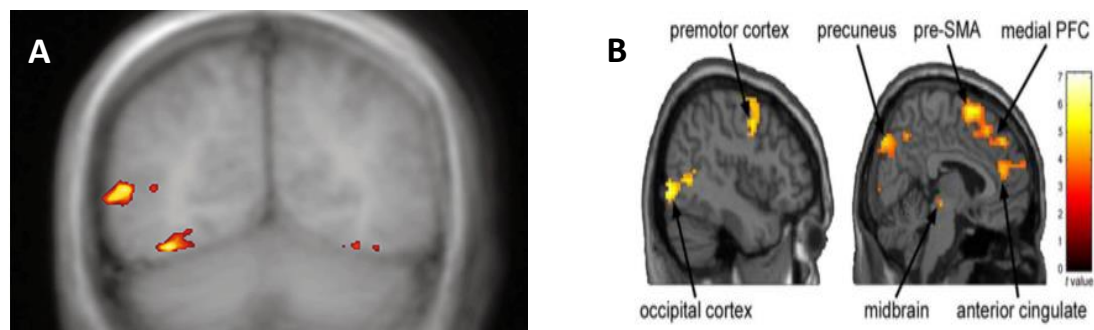
Figure 2 – Representative images of the activation of different regions of the PFC evoked during social hierarchy perception. A: The VLPFC responds to nonverbal cues of high social status. *Adapted from Allison, T., Puce, A. & McCarthy, G. Social perception from visual cues: Role of the STS region (2000);* **B:** The mPFC is recurently evoked in an unstable hierarchy setting. **Abbreviations:** SMA, supplementary motor area. *Adapted from Zink, C. F. et al. Know Your Place: Neural Processing of Social Hierarchy in Humans (2008).*

Inference of social rank through observation of pairwise contests also relies on mPFC function, as it was shown to be responsible for the learning of ranks, the estimation of a certain individual's position within the hierarchy and for keeping updated information about one's position in the hierarchy[52]. Another fMRI study investigated the neural basis behind the learning of social hierarchies through direct competition, revealing that the rmPFC is vital in tracking and updating the opponent's social status, while the vmPFC together with the ventral striatum forms a motivational network responsible for eliciting an affective meaning to winning and losing a competitive dispute[53]. These results show that previous social experiences can influence the activity of brain's motivational networks, evidencing an intricate relationship between social status and motivation, which in turn may influence future competitive disputes.

Lesion studies have reported that selective ablation of some of the PFC areas can result in impaired social behaviors, such as reduced processing of social status information in humans[43,54,55]. Particularly, lesions to the mPFC have been reported to cause loss of sensitivity to social cues[54], further supporting the role of this region in social hierarchy neuronal processing. In rodents, similar type of "loss-of-function" experiments have showed that an injured mPFC

results in decreased interest, loss of social memory and in a deficit in effort-based decision-making[56].

Focusing on a more molecular level, Wang *et al. (2011)*[29] questioned the consequence of promoting or silencing synaptic plasticity at the dmPFC of mice. By strengthening or weakening the mPFC excitatory synapses through the expression of AMPA-receptor subunit GluA4 or a GluA4 C-tail, respectively, they showed that it is possible to alter the social ranking of an already established hierarchy[29]. Strengthening the glutamatergic synapses of the dorsal PFC of subordinate mice lead to an increase in their ranks and also in the emission of vocalizations whilst the opposite was observed when weakening these synapses in dominant males[26]. Further observations that higher-ranked animals show stronger excitatory synaptic inputs in the mPFC highlight the involvement of this brain region in social hierarchy[26]. Indeed, AMPA-mediated amplitudes were increased in layer V pyramidal neurons of dominant animals when compared to low-ranked individuals[26]. Moreover, after tube-test encounters, dominant mice also displayed higher neuronal activation in the mPFC, as suggested by the increased number of c-Fos-positive neurons, particularly in the pre-limbic (PrL) region[26].

Another recent study, by Zhou H. *et al.* (2017)[27], tested the role of the dmPFC neuronal activity during tube test encounters. The results showed that the inhibition and activation of dmPFC neuronal activity have opposite effects on individual's appetence to initiate pushes and resist pushes with push-backs. Inhibition of dmPFC neuron activity also resulted in a drop of dominance rank, whilst its activation resulted in an increase in rank[27].

These studies demonstrate a direct correlation between mPFC activity and dominance status, suggesting a central role of this particular brain region in the regulation of social status in mice.

1.5 – The Role of the Striatum in Social Hierarchy Perception

As described so far, frontal regions of the brain, specifically the PFC, have been identified as key regions in neuronal processing of social hierarchies. Other brain regions, such as the basal ganglia and the limbic and paralimbic cortices, are commonly described to be involved with the generation and interpretation of emotions and also with processing reward stimuli, a role most commonly attributed to the striatum[57]. Most reports have implicated the striatum during mental processes such as interpretation of value and reward prediction within non-social contexts[58–62]. However, it is also suggested to be involved in the perception of social dominance in social contexts[14]. In this last case, a study done by Zink, *et al.* (2008) showed an increased striatal response was elicited when subjects won over higher-ranked human players rather than computer-based opponents or lower-ranked human opponents[14] **(Figure 3)**. These results dovetail with other studies suggesting higher sensitivity to reward in social competitive situations[63,64] and further suggests the striatum is involved in the greater reward anticipation that comes from beating higher-ranked opponents. Also importantly, this study showed that the striatum, specifically the ventral striatum, had greater activation when subjects were looking at higher-ranked human opponents, compared to facing a lower-ranked human opponent[14] **(Figure**

3). As such, this study was the first to successfully unveil a social component to the striatum, more specifically the involvement of the ventral striatum in social hierarchy perception.
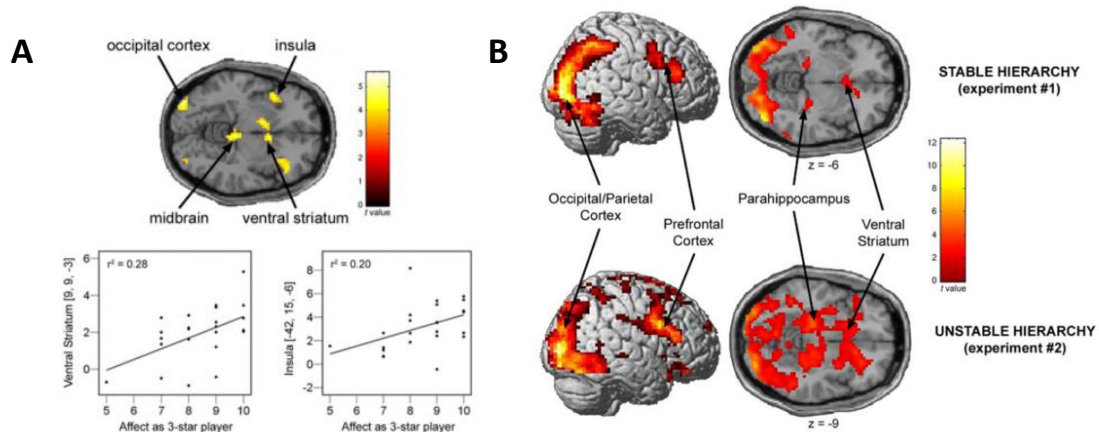
Figure 3 – The role of the ventral striatum in social dominance perception: A: Greater activation of the ventral striatum is elicited after beating a higher-ranked human opponent; **B:** Different ventral striatum activity registered during the perception of "superior player" faces versus "inferior player" faces. *Adapted from Zink, C. F. et al. Know Your Place: Neural Processing of Social Hierarchy in Humans (2008)*

1.6 – The Corticostriatal Circuitry Role in Social Hierarchy

As shown so far, both the PFC and the striatum have a role during social rank perception. These two brain regions are not dissociated and, together with other cortical regions, the thalamus and the rest of the basal ganglia (where the striatum is inserted) form a large neuronal interconnection of large-scale loops commonly designated as the Corticostriatal Circuitry, which major role is to assure proper forebrain function[65] **(Figure 4, A)**. Cortex and striatum connect in a well-defined, bidirectional manner, but with fundamental differences: from the cortex to the striatum communication is direct and monosynaptic, whereas striatum projections to the cortex are indirect, via downstream circuits, and polysynaptic[66–68].

Within this circuit, the mPFC strongly innervates the ventral striatum through projections that reach the nucleus accumbens (NAcc), a nucleus located in the ventral-most part of the striatum that acts as a gateway between this brain region and the frontal and temporal lobes of the cortex[69,70] **(Figure 4, B)**.
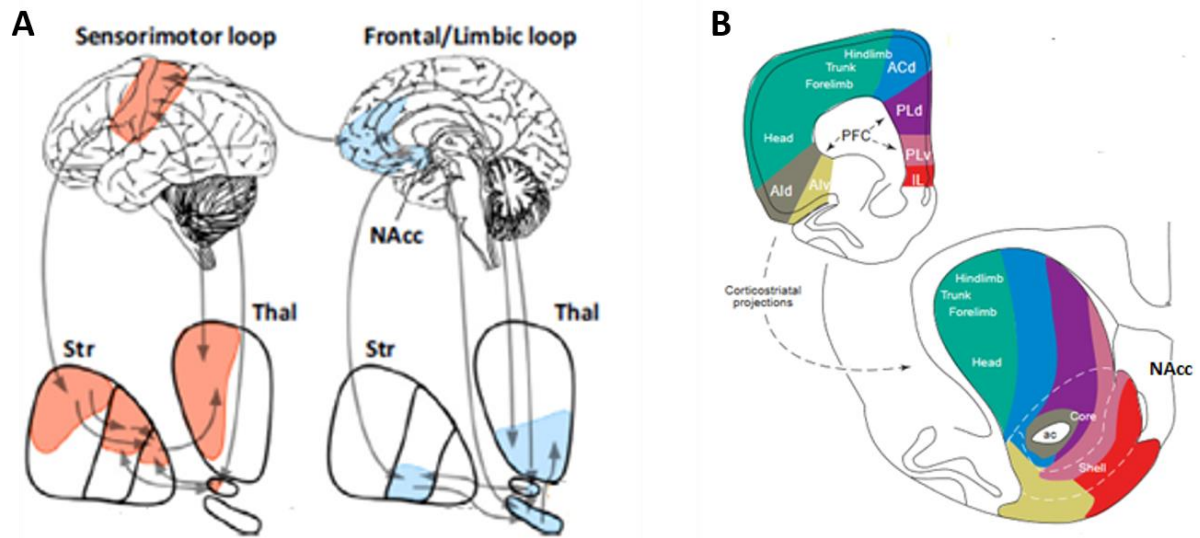
Figure 4 – Representative models of corticostriatal pathways, in Humans and Mice. A: Arrows broadly indicate how information is processed through these neuronal loops. *Adapted from Tobias U. Hauser et al. Computational Psychiatry of ADHD: Neural Gain Impairments across Marrian Levels of Analysis (2016)* [71]. **B:** Mice PFC regions project to corresponding striatal zones (same colour scheme) following a strict topographical organization. The different constituents of the mPFC (AC, PL and IL regions) follow this same organization to innervate the NAcc, in its core and shell regions. **Abbreviations:** NAcc, nucleus accumbens; Str, striatum; Thal, thalamus; ac, anterior commissure; ACd, dorsal anterior cingulate cortex; AId, dorsal agranular insular cortex; AIv, ventral agranular insular cortex; IL, infralimbic cortex; PFC, prefrontal cortex; PLd, dorsal prelimbic cortex; PLv, ventral prelimbic cortex. *Adapted from Pieter Voorn et al. Putting a spin on the dorsal–ventral divide of the striatum (2004)* [72].

In addition to the role in social hierarchy perception unveiled by Zink, *et al.* (2008), the NAcc also has a role in integrating emotional and mnemonic signals from the frontal and temporal lobes within the limbic system and converting them in a corresponding motor response [73,74]. It has been extensively linked to the regulation of motivational aspects of behavior, such as effort-based decision and choice making [75,76], which underlie initiative and/or effort exertion on the part of the animal. Specifically, the projections between the NAcc and the PFC are described to drive mice to reach motivational goals, whether that be obtaining a certain reward or keep off aversive stimuli [77–79]. Strikingly, previous studies, focusing on the identification of brain regions involved in social decision-making, have evidenced a functional overlap between regions that respond to dominance cues and social rank perception (including the PFC) and regions involved with traits such as motivation to win or to avoid losing (eg: PFC, amygdala and ventral striatum) [35,80–89] **(Figure 5)**.
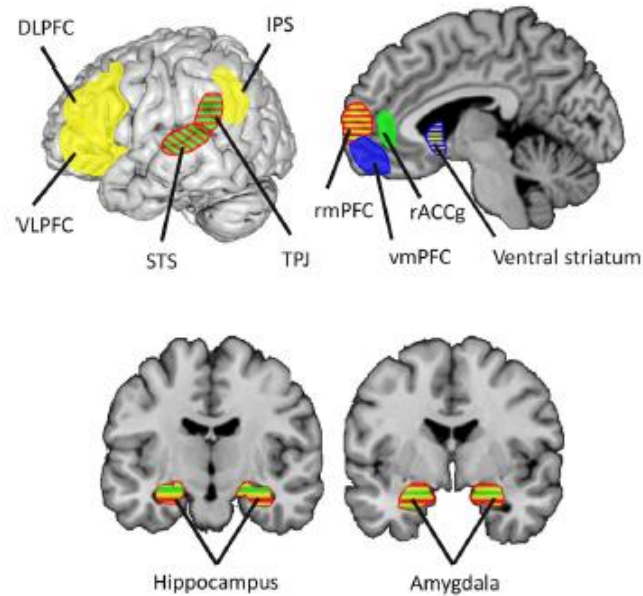
Figure 5 – Representative image of the overlapping in brain regions identified in Human Neuroimaging Studies. The brain network involved in social rank perception (yellow), learning of hierarchies through observation (green) and competition (red) and the motivational network (blue). **Abbreviations:** DLPFC, dorsolateral prefrontal cortex; IPS, intraparietal sulcus region; rACCg, rostral anterior cingulate gyrus; rmPFC, rostromedial prefrontal cortex; STS, superior temporal sulcus region; TPJ, temporo-parietal junction; VLPFC, ventrolateral prefrontal cortex; vmPFC, ventromedial prefrontal cortex. *Adapted from Chen Qu et al. An Integrative Interdisciplinary Perspective on Social Dominance Hierarchies (2017)*[90].

Recently, Amadei *et al.* (2017) explored the role of the projections between mPFC and NAcc in sociosexual interactions, and whether it had influence over female mice's expression of affiliative behavior towards a partner, since pair bonding recurrently activates the brain's reward system[91–93]. The results show that a rhythmic activation of this circuit, and its consequent strengthening, within a social context can, in itself, induce and accelerate a preference towards a sexual partner, without the need for mating rituals. Importantly, this study was the first to successfully show the recruitment of the brain's reward systems during social interactions and, more importantly, implicate them during mice behavior in social contexts.

Since dominant mice show stronger excitatory synaptic inputs in their mPFC[26] **(Figure 6)**, we hypothesize that mPFC outputs onto other downstream brain regions, such as the NAcc, may also be stronger in more dominant animals.
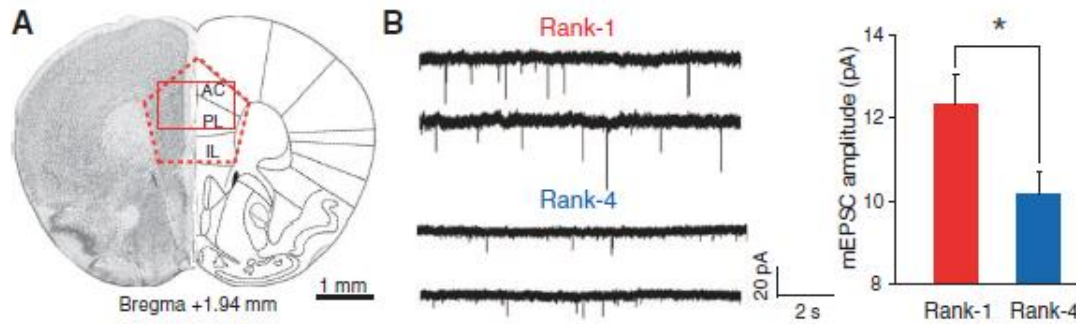
Figure 6 - Higher ranked animals showed increased amplitude in excitatory pre-synaptic currents (mEPSC) in their mPFC neurons. A: Visual representation of where the recordings were made (between the anterior cingulate and pre-Limbic regions of the mPFC); **B:** Representative tracing of the recordings made (left) and sum of the results gained from a total of 60 neurons (right). Adapted from *Wang, F. et al. Bidirectional control of social hierarchy by synaptic efficacy in medial prefrontal cortex (2011).*

Although not extensively studied, the connection between mPFC and NAcc has been described to modulate behavior during social interactions[94]. Furthermore, it can be hypothesized that stronger synaptic proprieties in the mPFC-NAcc connectivity propel an individual's propension to reach higher ranks in its social group. As seen this far, frontal cortex regions, namely the mPFC, and the ventral striatum have been described for being involved in social hierarchy processing at different levels of cognition but also with motivational and effort-based aspects of behavior. As motivation and reward processing can be essential requirements for sustained winning in social contests, such as tube test encounters, future studies should focus on unveiling the role of these neuronal projections in these social dominance behaviors.

Specific Objectives

With this work we are interested in functionally and anatomically map the connections between the mPFC and the NAcc in the context of social dominance namely through:

- retrograde cholera toxin labelling;
- whole-cell patch clamp in acute brain slices.

We also aim at the manipulation of this circuit activity through optogenetics, namely through:

- stereotactic delivery of AVV viral vectors expressing channelrhodopsin-2 in the NAcc and stimulation with fibers in the mPFC to manipulate this circuit;
- functional studies to assess if we can change a pre-established social hierarchy in mice.

Chapter 2| Methods and Materials

2.1 - Animals

All experiments were performed with male C57/BL6 mice with 2-5 months old, acquired from Charles Rivers. Animals were kept at the vivarium of the Faculty of Medicine, University of Coimbra in groups of 4 per cage and in a 12 hours light/dark cycle in temperature- and humidity-controlled rooms, with food and water provided *ad libitum*. Upon arrival, animals were acclimatized to the vivarium room for a week before any experiments took place. Before behavioral testing, animals were handled for 4 consecutive days. After the surgical procedure, animals were kept in the vivarium single-housed, as to prevent cage-mates from tampering with the implant. Animal identification was performed by subcutaneous injection of green and/or black dyes in the paws. All experiments were carried with the approval of the animal ethics committee of the Center for Neuroscience and Cell Biology, University of Coimbra (ORBEA), the approval of the Portuguese "Direção Geral de Alimentação e Veterinária" (DGAV) and in accordance with EU directives regarding animal use in research.

2.2 - Electrophysiology Recordings

2.2.1 - Hierarchy Establishment

Before tube test encounters, every animal was subjected to a 3-day tube test habituation period that consisted in them walking through the narrow tube (a transparent plastic tube with 24cm length and 2.4cm diameter) 10 times, each day. After that, animals were tested in a round-robin match arrangement until a stable social hierarchy could be defined, i.e., all ranks remained stable for a minimum period of three days. Each round was designed so that all animals face each other, and the time between encounters allowed similar resting periods. The encounter started by introducing two mice at each end of the tube and ended when one of the animals exited the tube (with all 4 paws) for at least 4 seconds. The winning animal was scored as the dominant mouse of the pair. Animals ranked in opposite ends of the stable hierarchy (the most dominant and the most subordinate) were sacrificed for whole-cell patch clamp recordings.

All behavioral experiments were performed during the light cycle. Animals were placed in the behavioral room for at least 2 hours prior to testing to allow acclimatization. Camera recordings were performed in side view and video-taping was scored offline using Cineplex Editor (Plexon).

2.2.2 – Brain sectioning and solutions

Brain slices for recordings were prepared using the *N*-methyl-D-glucamine (NMDG) protective recovery method of brain slice preparation, as described by Jonathan Ting *et al*[103]. This method involved the perfusion, sectioning and recovery of acute brain slices in NMDG-HEPES artificial cerebrospinal fluid (aCSF), whereas recordings are performed with standard aCSF solutions (see composition in **Table 1**).

Table 1 - Composition of NMDG-HEPES aCSF and recording aCSF solutions.

Compound	NMDG – HEPES aCSF		Recording aCSF	
	MW	g/Liter	MW	g/Liter
NMDG	195.22	19.46	-	-
NaCl	-	-	58.44	7.25
Kcl	74.55	0.19	74.55	0.19
NaH_2PO_4	138.00	0.17	138.00	0.17
$NaHCO_3$	84.01	2.52	84.01	2.02
HEPES	238.31	4.77	238.31	1.19
Glucose	180.20	4.51	180.20	2.25
Sodium Ascorbate	198.00	0.99	-	-
Thiourea	76.12	0.15	-	-
Sodium Pyruvate	110.04	0.33	-	-
After Solubilization				
$MgSO_4.7H_2O$	246.48	5mL	246.48	1mL
$CaCl_2.2H_2O$	147.01	0,5mL	147.01	2mL

The solutions were prepared with milliQ-H_2O, pH was adjusted to 7.3-7.4 (with 10 M HCl in the case of NMDG-HEPES aCSF) and osmolality was measured and adjusted to the interval of 300-310 mOsm/kg. Solutions were filtered, kept at 4°C and used during two consecutive days.

2.2.3 – Recordings

Coronal acute brain slices (300 µm thick) containing the NAcc **(See Supplementary Figure 1)** were prepared by an experimentalist blinded to the phenotype of the animals. Before brain dissection, mice were put under deep anesthesia with isofluorane (IsoFlo) and perfused with an oxygenated (95% O_2: 5% CO_2 mixture) NMDG-HEPES solution. Per brain, 3-4 consecutive slices were obtained using a vibratome (Leica VT1200s, Leica Microsystems, USA) and immediately placed for recovery at 32°C for 8 minutes before being transferred to a holding chamber with aCSF. Slices were kept in oxygenated aCSF (at room-temperature) for at least an hour before the recordings.

Slices were placed in a recording chamber, and constantly perfused at a rate of 1-2 mL/min, at room temperature. Nucleus accumbens and individual medium spiny neurons (MSN) were visualized with a microscope Axio Examiner D1 microscope (Zeiss, Germany) equipped with IR-DIC optics and a Q-capture Pro 7 camera (Qimaging, Canada). MSNs were selected for recording according to the shape of their cell bodies and a relatively higher membrane capacitance than that of interneurons[95].

All recordings were performed with an internal solution with the following composition (mM): $CsMeSO_3$ 107, CsCl 10, NaCl 3.7, TEA-Cl 5, HEPES 20, EGTA 0.2, Lidocaine N-ethyl chloride 5, ATP-Mg salt 4, GTP-Na salt 0.3[95]. pH was adjusted to 7.3-7.4 (with CsOH) and osmolarity was measured and corrected to 295-300 mOsm with $CsMeSO_3$. Cells were patched with borosilicate glass recording electrodes (3-5 MΩ; Science Products) filled with internal solution. Recordings of α-amino-3-hydroxy-5-methyl-4-isoxazolepropionic acid (AMPA) mediated miniature excitatory post-synaptic currents (AMPA-mEPSC) were performed in the presence of TTX (10 μM), bicuculline (25 μM) and D-APV (20 μM) in the extracellular solution. Spontaneous excitatory post-synaptic currents (sEPSC) were measured in the absence of drugs in the extracellular solution. Both types of recordings were performed under voltage-clamp at -70 mV of holding voltage. For each animal, each of the two types of recordings were performed using one slice per type, while randomizing the slice and the order of the type of recording along the session.

2.2.4 – Quantification

Synaptic events were quantified using Clampfit 10.7.0 software (Molecular Devices). The data was organized using a costume script on Matlab 2016a (Mathworks) and statistical analysis was performed using Prism (Graphpad). Cells included in the analysis had a series resistance below 20 MOhm and a variation of series resistance below 20% of the initial value. For each recording the first 30 consecutive events were analyzed.

2.3 - Neuroanatomical Circuit Mapping

Anatomical mapping of the mPFC-NAcc connectivity was accomplished with the use of the neurotracer Cholera Toxin sub-unit B (CTB) fused to Alexa Fluor 488 (ThermoFisher). CTB working solution (0.1%) was obtained after dissolving 100micrograms in 0.1mL of a PBS buffer (1mg/mL, 0.1% wt/vol), according to ThermoFisher protocols. The delivery methodology was adapted from a protocol described previously[96].

2.3.1 - Stereotaxic Surgery
2.3.1.1 - Preparation
Animal weight was registered, the surgical surface was disinfected with bleach followed by Ethanol 70% and tools sterilized by autoclave.

2.3.1.2 – Anesthesia and fixation of the animal to the stereotaxic frame

The animal was placed in a tightly sealed chamber and deeply anesthetized with 5% vaporized isoflurane/O_2 mixture until loss of righting reflexes. It was then transferred to a breather, where vaporization was reduced to 2% and depth of anesthesia was tested using the paw pinch test (withdrawal reflex). Air flow was kept at around 1L/min and with a 1.5-2% isoflurane/O_2 mixture. The animal received preemptive anti-inflammatory and analgesia injections (Meloxicam 1mg/kg or Carprofen 5mg/Kg intra-peritoneally and Buprenorphine 0.05mg/kg sub-cutaneous). Ophthalmic ointment was applied to prevent eye drying and the head was shaved off with a shaver and/or depilatory cream.

A heating pad was set up and placed on the stereotaxic frame to keep the animal's body temperature stable. While supporting the head of the animal, one of the ear bars was locked into the external auditory meatus. This step was repeated for the opposite ear bar until the head of the animal was firmly secured. Because this procedure involves recovery from surgery, only non-rupture ear bars with a wide-angle tip were used to avoid injuring the tympanic membrane. Then, the incisor bar was inserted into the mouth of the animal while holding its jaw open with a pair of forceps. The incisor bar was locked by applying pressure into the bridge of the animal's nose by sliding in a vaporizing mask.

2.3.1.3 – Opening the scalp for craniotomy

The scalp of the animal was disinfected with betadine and 70% ethanol rinses (alternated and repeated three times). A saline solution was intraperitonially injected to keep the animal from dehydrating during surgery (10 mL/kg). A drop of lidocaine + epinephrine solution was applied onto the periosteum (the amount given should not exceed 7mg/kg, approximately 8-9 microliters) to prevent excessive bleeding or pain. A scalpel was used to make an incision along the midline and expose the skull. The skull was then cleaned with cotton swabs immersed in hydrogen peroxide followed by sterile PBS to disinfect and highlight the cranial sutures.

2.3.1.4 - Craniotomy

Using a nanoinjector (World Precision Instruments) attached to the stereotaxic frame, a glass micropipette was filled with a gentian violet dye. By lowering the tip of the micropippete until it gently touches the skull, bregma and lambda sites were marked to ensure the proper fixation of the animal and help to determine the craniotomy and injection places. The bregma was identified as the point of intersection of the sagittal suture with the curve that best fits the coronal suture, with the lambda being the midpoint along the lambdoid suture **(See Supplementary Figure 2)**. To ensure that the skull was flat, Bregma and lambda were adjusted to the same dorsal–ventral (DV) coordinate by adjusting the height of the nose clamp on the stereotactic frame. The same alignment was then performed in the rostro-caudal and medio-lateral axis by adjusting the height of the ear bars. The RC and ML coordinates of the injection sites were then marked in the skull with the gentian violet dye-filled glass micropipette. A hand-held drill was used to reveal the surface of the brain, by opening small craniotomies wide enough to allow a glass micropipette through.

2.3.1.5 – CTB injection

Stereotaxic targeting of the NAcc (+1.5mm RC, +0.8mm ML, -4.0mm DV) was accomplished using the Bregma as the reference point. The nanoinjector, with the glass micropipette now filled with CTB working solution, was tilted 10° outwards in the rostro-caudal axis **(See Supplementary Figure 3)** and lowered until it reached the surface of the exposed brain. From there, it was lowered at a rate of approximately 1mm/min until it reached the final depth of 4.0mm, where 2 injections of 69nanoliters were done for each hemisphere.

After the injections we performed, the drill holes were covered using bone-wax (Braun) and the scalp sutured.

2.3.1.6 – Post-surgery recovery

During the first hours of the post-surgical recovery period, animals were placed in a clean cage over a heating pad and provided food soaked in water (containing minocycline 0.1mg/ml). Buprenorphine (0.05mg/kg, SC) was administered again within 24h and 2 injections of Meloxicam (1 mg/kg, IP) were given in the first and second days after surgery. Mice were monitored daily for signs of distress such as weight variations or reduced locomotion and let to recover for at least 7 days.

2.3.2 – Histology and Image Processing

Animals were deeply anesthetized and perfused with 1x phosphate buffered saline (PBS) solution (10x PBS: 87,6 g of NaCl (Acros); 32,5 g of $Na_2HPO_4.7H_2O$ (Fisher); 4 g of KH_2PO_4 (Fisher)) and with a 4% paraformaldehyde (PFA) solution (4 g of PFA (Fisher) in 100mL of 1x PBS), and stored in 30% sucrose (30 g sucrose (Fisher) in 100 mL of 1x PBS) for cryopreservation. Coronal brain slices were cut with 50μm (Leica VT1200s, Leica Microsystems, USA) and mounted on Mowiol medium (Mowiol 4-88, Sigma) with DAPI (1:1000). Images were obtained using an Axio Imager 2 microscope (Zeiss, Germany).

2.4 - Optogenetic Manipulation of Corticostriatal Projections

2.4.1 - Implantable Optical Fibers

Implantable optic fibers were built with material from ThorLabs and following standard procedures[97]. Briefly, a striped optic fiber (Ø 200μm / 0.39 NA) was glued with cyanoacrylate adhesive (Loctite), to either a 1.25mm Multimode LC/PC stainless steel ferrule (Ø 231μm) or a ceramic LC MM ferrule (Ø 230μm). The exposed end of the optic fiber was scored by holding a sapphire coated blade perpendicular to it, in a single motion, and cleaved to 2mm in length. The ferrule' convex surface and the optical fiber were then polished with increasing fine grades of polishing paper (ThorLabs).

2.4.2 – Stereotaxic Surgery

Adeno-associated viral construct coding for Channelrhodopsin (AAV.hSyn.hChR2(H134R)-EYFP), or ChR2, was bilaterally delivery to the NAcc and optical fibers implanted bilaterally in the mPFC using a stereotactic method described previously[98]. The core of the procedure is the same as described for the CTB injections, with some alterations, detailed below:

2.4.2.1 - Craniotomy

To increase the bond strength between the skull and the dental cement used for fixation of the Optical Fibers, the skull was scored over the target area using a hand-held drill in horizontal movement and slight downward pressure. The same hand-held drill was then used to open small craniotomies in the coordinates intended for both viral injection and optic fiber placement. An additional two holes were drilled to implant sterile self-tapping anchor screws (M1.2 x 4). The screws were implanted until contact with the dura and further fixated with VersaGlue PX-40 (Harvest Dental). These screws create additional adhesion surface for the cement application, further securing the implant to the head of the animal.

2.4.2.2 – ChR2 injection

Stereotaxic targeting of the NAcc (+1.5mm RC, +0.8mm ML) was accomplished as detailed previously. The glass micropipette was filled with 2 μl of ChR2-coding AAV's solution (1.03e14 GC/mL) and tilted 10° outwards in the rostro-caudal axis **(See Supplementary Figure 3)**.
To maximize infection in the NAcc, viral injections were performed at three different depths (DV -4.3, -4.1 and -3.7mm). Two injections of 69nL were performed at each depth, separated by 15s. Before ascending to the next injection site, a waiting period of 5min to prevent backflow. After the third and last injection, a final waiting period of 10min was given.

2.4.2.3 - Optical fibers Implantation

Stereotaxic targeting of the mPFC (+1.8mm RC, +0.6mm ML, -1.3mm DV) was accomplished as detailed previously. An adapter for implantable optical fibers was attached to the stereotaxic frame and tilted 10º outwards in the medio-lateral axis **(See Supplementary Figure 3)**. Placing the fiber cannulas with this angle facilitates the future attachment of the optic fiber cables.
The stereotaxic arm with the implantable optical fiber (1.25mm Multimode LC/PC SS Ferrule Ø231μm or Ceramic LC MM Ferrule 230μm, from ThorLabs) was then lowered into the intended depth at a rate of approximately 1 mm/min.

2.4.2.4 - Cement Application

The skull was thoroughly dried using cotton swabs. A thin layer of self-adhesive resin cement (Maxcem Elite™, Kerr) or dental cement (Ketac Cem, 3M) was used to cover the exposed surface of the skull, around the anchor screws and on each side of the fibers. Once the first layer polymerized, the fibers were released from the stereotaxic arm and more cement was applied to further secure the implants in place. Finally, a dental acrylic mixture was applied (Scheu Dental) to protect both the cement and the implant. Lastly, 3-action antibiotic ophthalmic ointment (Meocil, Edol) was applied on the eyes and exposed skin flaps.

2.4.3 – Behavioral Testing

As described before, after applying a 3-day habituation period, animals were tested in a round-robin match arrangement until a stable social hierarchy could be defined. This time, a transparent plexiglass tube (33cm length, Ø 3cm) with a 12mm open slit on top was used. The open slit allows for the attachment of optic fiber cables to the animal during tube test encounters.

2.4.4 – Neuronal Stimulation in the Tube Test

To guarantee adequate viral propagation, photo stimulation of the targeted neuronal projections was performed at least 4 weeks after viral injection, with light being delivered to the mPFC through an external optical fiber cable (Ø 200 µm, NA: 0.39) that couples to the previously implanted optic fiber through a sleeve. The cable is coupled to a 465-nm light source (PlexBright LED, Plexon). Light frequency was controlled with a pulse generator (PlexBright LD-1, Plexon) connected to an Arduino board running custom-written code. Light intensity was measured to approximately 6mW at the fiber tip. After hierarchy establishment, lower-ranked animals were stimulated during tube test encounters. Different photo-stimulation strategies were implemented. First, we used unilateral continuous photo-stimulation, from the moment the animal enters the tube until it leaves. We also used bilateral photo-stimulation only after a tube test win, using either continuous or 100Hz phasic modulated light protocol, as previously described[99].

2.4.5 - Tube Test Behavioral Decoding

Tube test videos were analyzed frame by frame using Cineplex Editor (Plexon), from the time-frame immediately after release of the animals until 4 seconds after one of the animals exited the tube entirely. Distinct behaviors during tube test encounters were categorized as pushing, stillness, resistance (both when pushing or being pushed) and retreating **(See Supplementary Figure 4)**.

2.4.6 – Histology and Image Processing

Stimulated animals were sacrificed after being placed under deep anesthesia. The brains were then perfused, cryopreserved, sliced, mounted and imaged as described before.

2.5 - Validation of Photo-induced Activation of Neuronal Projections

To confirm the photo-induced mPFC-NAcc neuronal projection activity, we performed an essay based on the detection of the immediate early gene cFos. For that, we photo-stimulated the mPFC of animals injected in the NAcc with the same ChR2 viral constructs as mentioned before. Light stimulation at 465nm was applied for two 1-minute periods with a 2-minute interval in between. After 90 minutes, animals were sacrificed and the brains perfused, cryopreserved and sliced as described before. The immunohistochemistry essay started by washing the brain slices 3 times, 20 minutes each, with 1x PBS followed by a blocking step during 1 hour at room-temperature, with a blocking solution (5% normal goat serum; 2% albumin bovine; 0.2% Triton-X). After incubation with blocking buffer solution containing the primary antibody against c-Fos (Abcam, 1:500) for 48 hours at 4ºC, slices were again washed 3 times with 1x PBS and then incubated overnight at 4ºC with blocking buffer solution containing the secondary antibody (Life Technologies, 1:1000, Alexa-568). Finally, slices were mounted and imaged as described before.

Chapter 3| Results

3.1 - Electrophysiology Recordings

To functionally characterize mPFC-NAcc neuronal projections role in social dominance, we performed *in vitro* whole-cell patch clamp recordings of brain slices containing the NAcc, from animals which hierarchical rank was previously assessed. **(Figure 7)**.
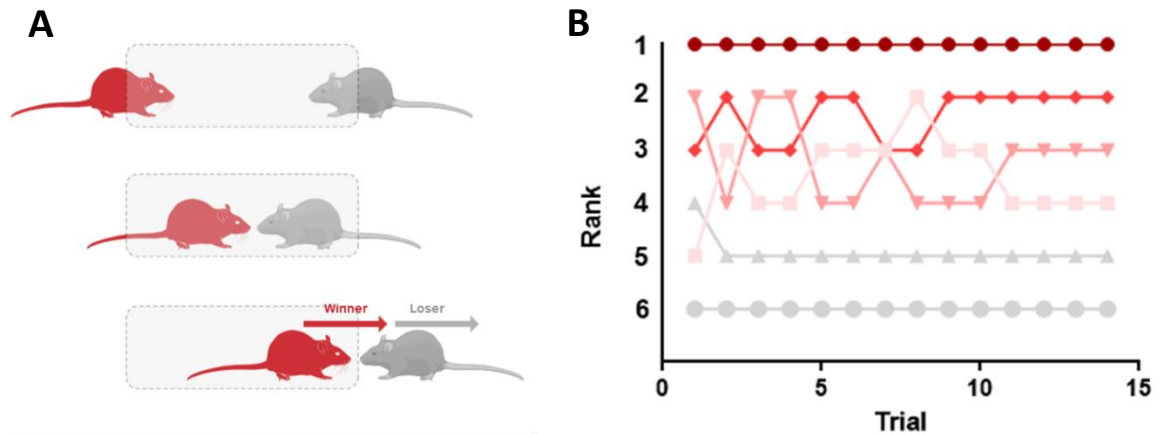
Figure 7: Tube test match encounters were performed until a stable hierarchy could be defined. A: Tube test winner mice were scored as the dominants of the pair. **B:** Hierarchy establishment with rank alteration along 14 trials.

For each recording session, measures were performed in pairs of mice with (stable) ranks in the opposite ends of the hierarchy. Measurements of spontaneous excitatory postsynaptic currents (sEPSCs) in individual MSNs were performed and results were normalized for each pair of individuals **(Figure 8).**
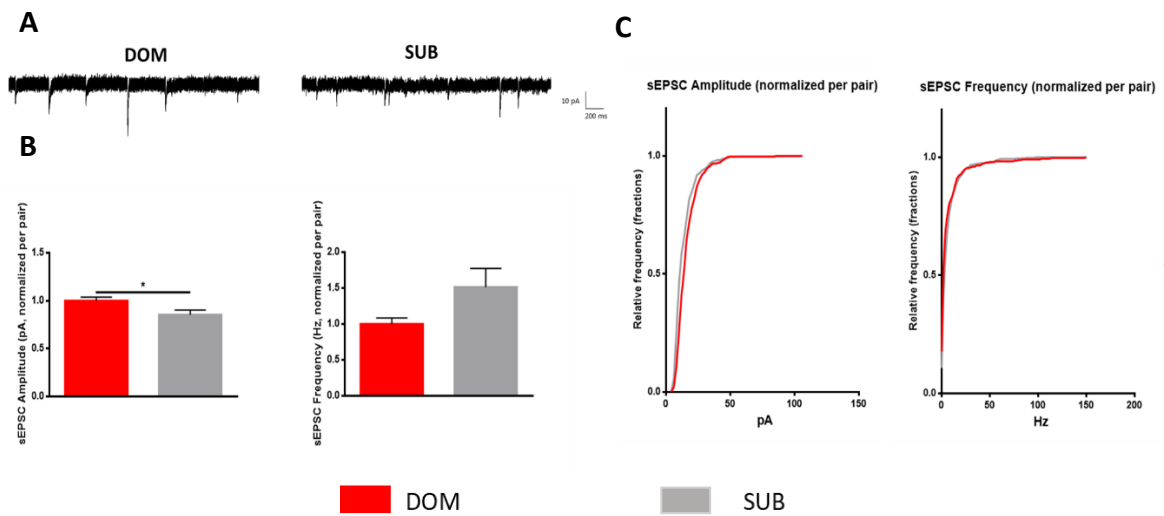
Figure 8: Dominant animals show increased sEPSC amplitude in NAcc neurons. A: sEPSC traces from dominant and subordinate neurons. Scale bar 10pA, 200ms; **B:** significant increase in sEPSC amplitude and non-significant differences in sEPSC frequency (results were normalized for each dominant/subordinate pair, dominant = 12 cells and subordinates = 15 cells). The statistical comparisons were performed using Mann-Whitney U Test. Statistical significance was set at *P<0.05, **P<0.01, ***P<0.001. Data are presented as means ±SEM; **C:** cumulative distribution of sEPSC amplitude and frequency.

Our results show a significant increase in the amplitude, but not in the frequency, of spontaneous sEPSCs in MSNs from the NAcc of dominant animals **(Figure 8)**. Additionally, measurements of monosynaptic AMPA-mediated mEPSCs were performed and results normalized for each pair of individuals **(Figure 9)**.
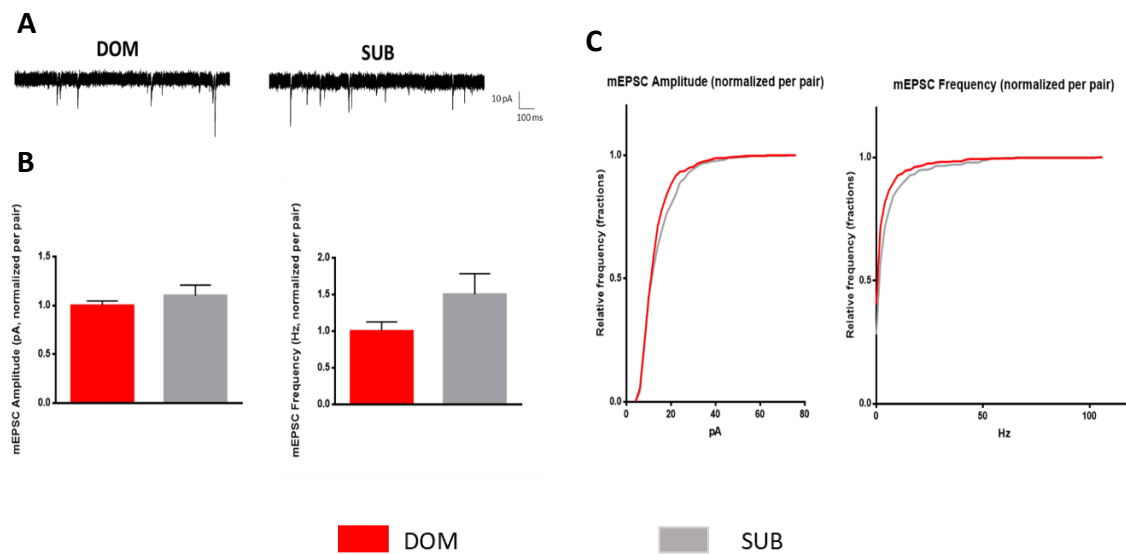
Figure 9: No differences in AMPA-mEPSCs recordings between dominant and subordinate animals were observed A: mEPSC traces from dominant and subordinate neurons. Scale bar 10pA, 100ms; **B:** Unaltered mEPSC amplitude and frequency (results were normalized for each dominant/subordinate pair, dominant = 15 cells and subordinates = 13 cells); **C:** cumulative distribution of mEPSC amplitude and frequency.

AMPA-mediated mEPSCs were unaltered, in amplitude or frequency, as our results show no statistical difference in either of these parameters **(Figure 9)**.

3.2 - Neurotracer Circuit Mapping

To anatomically map the mPFC-NAcc neuronal projections, we took advantage of a commercially available neuroanatomical tracer conjugated with a green fluorophore. The tracer was delivered to the NAcc and fluorescence was assessed throughout the whole brain, with particular interest in the mPFC. The representative images shown below were selected from brain regions where fluorescence was found. Assuming a correct delivery of the tracer, fluorescent signal was to be expected in the NAcc, which served as the injection site **(Figure 10)**.
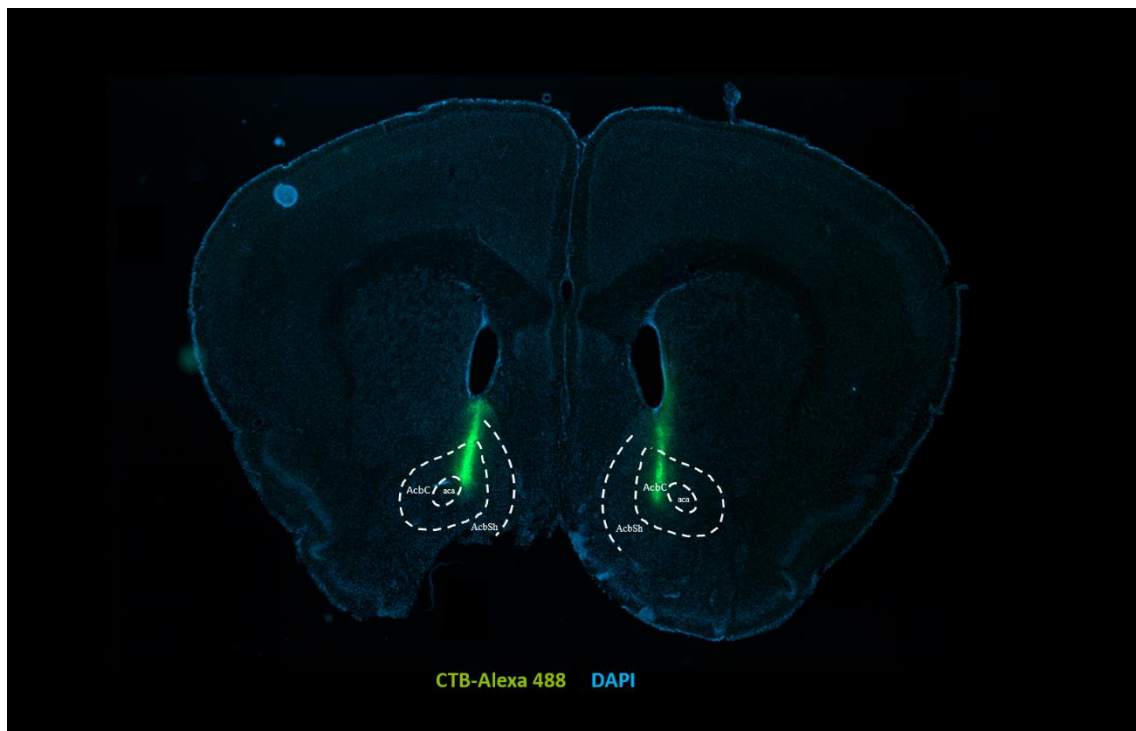
Figure 10: Successful injection of CTB in the NAcc. The figure shows the injection site (NAcc) labelled with the tracer's fluorescent signal (green), Bregma 1.18mm. **Abbreviations:** aca, anterior commissure; AcbC, nucleus accumbens, core region; AcbSh, nucleus accumbens, shell region.

In Figure 10 we show that the NAcc region was successfully reached, in both hemispheres. We next identified the brain regions where fluorescent signal was present via retrograde labelling. The rostral-most region of the brain with signal was the mPFC region, where labelled cells were observed in the anterior cingulate, pre-limbic and infra-limbic cortices **(Figure 11)**.
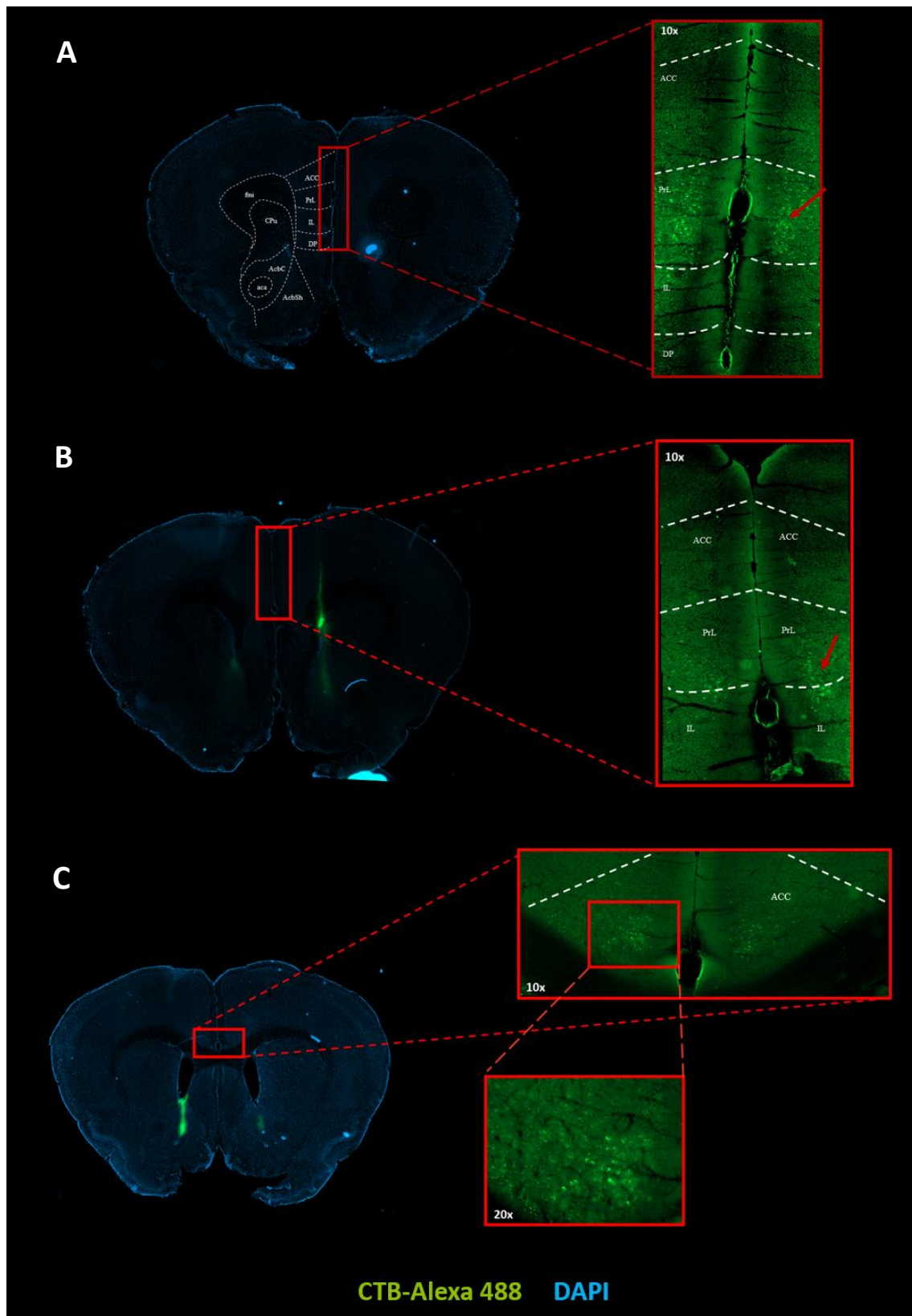
Figure 11: Tracer injection in the NAcc labells cells in the mPFC. The figure shows representative images of fluorescent signal in the mPFC, with close-up on labelled cells (red arrows) present in the anterior cingulate, pre-limbic and infra-limbic cortices. **A:** Bregma 1.70mm; **B:** Bregma: 1.54mm; **C:** Bregma 0.98mm. **Abbreviations:** aca, anterior commissure; AcbC, nucleus accumbens, core region; AcbSh, nucleus accumbens, shell region; ACC, anterior cingulate cortex; CPu, caudate putamen (striatum); DP, dorsal peduncular cortex; IL, infra-limbic cortex; fmi, forceps minor of the corpus callosum; PrL, pre-limbic cortex.

Togehter, our results show labelled cells in every region of the mPFC, which are found in greater number in both anterior cingulate and pre-limbic cortices, but nevertheless limited in number and circunscript to the upper-most part of the infra-limbic cortex **(Figure 12)**.

Moving to more caudal region of the brain, fluorescent signal was particularly distinctive in the thalamus region, right below the brain's third ventricle **(Figure 13)**.
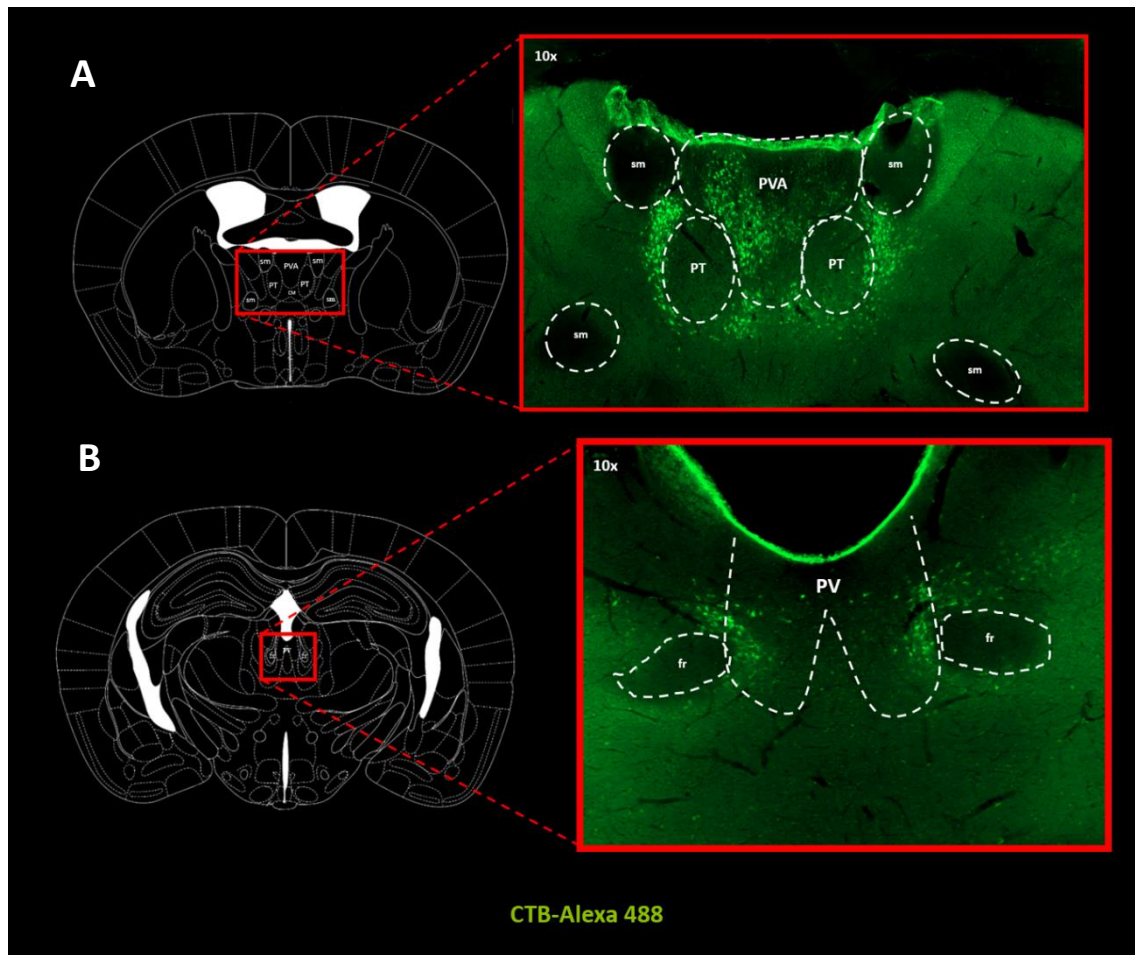
Figure 12: Tracer injection in the NAcc results in labelled cells in the paraventricular region of the thalamus. Figure shows close-up images of fluorescence signal in the thalamus. **A:** thalamus' anterior region (Bregma -0.46mm); **B:** thalamus' posterior region (Bregma -2.46mm). **Abbreviations:** CM, central medial thalamic nucleus; fr - fasciculus retroflexus; PT, paratenial thalamic nucleus; PV, paraventricular thalamic nucleus; PVA, paraventricular thalamic nucleus anterior part; sm, stria medullaris of the thalamus.

The tracer signal detected in the thalamus appears to follow the paraventricular thalamic nucleus (PV), in the anterior to posterior axis **(Figure 12)**.

Finally, the caudal-most part of the brain where fluorescence signal was found corresponded to the basolateral amygdala **(Figure 13)**.
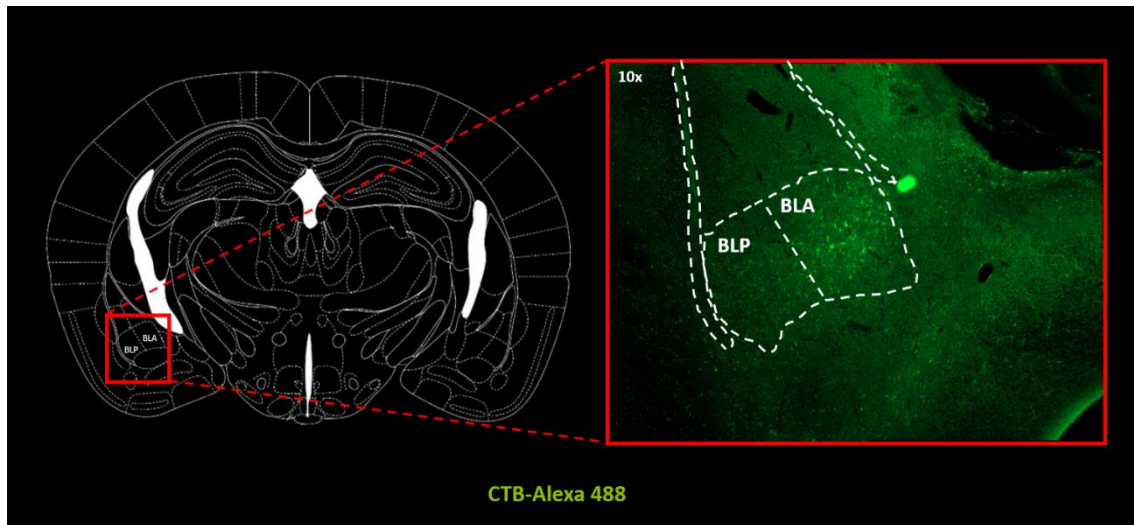
Figure 13: Tracer injection in the NAcc labels cells in the anterior basolateral amygdala. Figure shows a close-up image of labelled cells in the BLA region (Bregma -2.06mm); **Abbreviations:** BLA, basolateral amygdaloid nucleus, anterior part; BLP, basolateral amygdaloid nucleus, posterior part.

Detailed assessment of this signal suggests that it is circunscript to the anterior part of the basolateral amygdala **(Figure 13)**.

Together, our results show that the main areas projecting into the NAcc include the prelimbic and infralimbic areas of the prefrontal cortex, the paraventricular thalamic region and the basolateral amygdala. This convergence of information inputs signals from top-down cortical control (mPFC), but also sensory processing areas (thalamus)[100–103] and emotional valence (amygdala)[104,105] that converge onto the ventral striatum. This suggests the NAcc is particularly well positioned to assess and modulate information responsible towards selection of behavior programs in a region that is also involved in reward circuits.

3.3 - Optogenetic Manipulation of Corticostriatal Projections

To tackle if the modulation of corticostriatal projections using channelrhodopsin-based optogenetic techniques could alter a previously established hierarchy, we designed a set of experiments to stimulate lower-ranked individuals in a social hierarchy, aiming to increase their position. Animals' hierarchical rank was assessed by round-robin tube test encounters, as previously described, before an optogenetic stimulation protocol was applied. During these encounters, the stimulated mouse and its dominant opponent were video-monitored so that specific behaviors could be identified and quantified. Encounters duration was also measured. The first stimulation protocol tested was performed unilaterally and throughout the entire duration of the tube test encounter, from the point of release until the end of the encounter **(Figure 14)**.
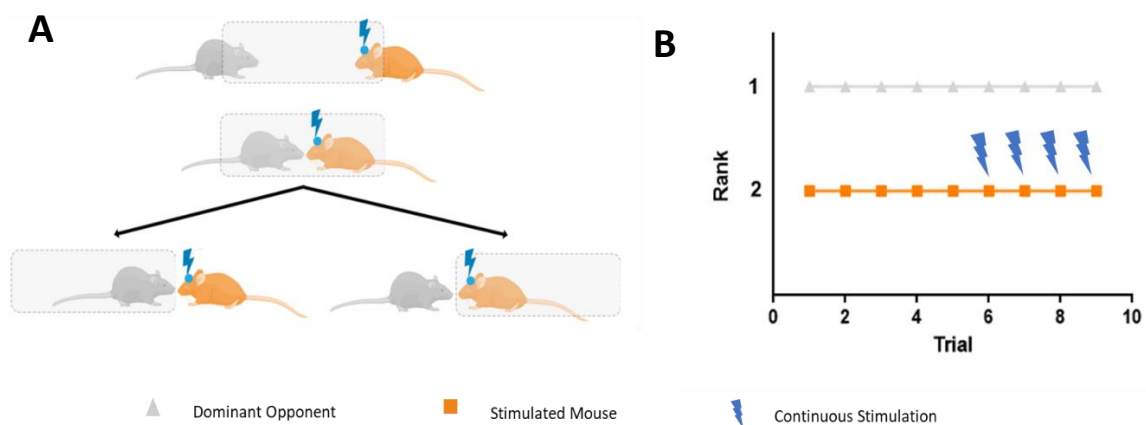
Figure 14: Unilateral and continuous stimulation of the lower-ranked mouse did not produce a positive rank switch. **A:** The lower-ranked animal was stimulated throughout the encounter, win or lose; **B:** Rank monitorization along 9 trials (each trial corresponds to one day and one encounter). The lower-ranked individual was unilaterally stimulated in the last 4 encounters;

Whether win or lose, the lower-ranked individual received unilateral and continuous stimulation throughout the encounter **(Figure 14, A)**. The stimulation protocol was repeated for four consecutive days but never produced tube test winning **(Figure 14, B)**. Trials with and without stimulation ("Hierarchy Assessment") were compared **(Figure 15)**.
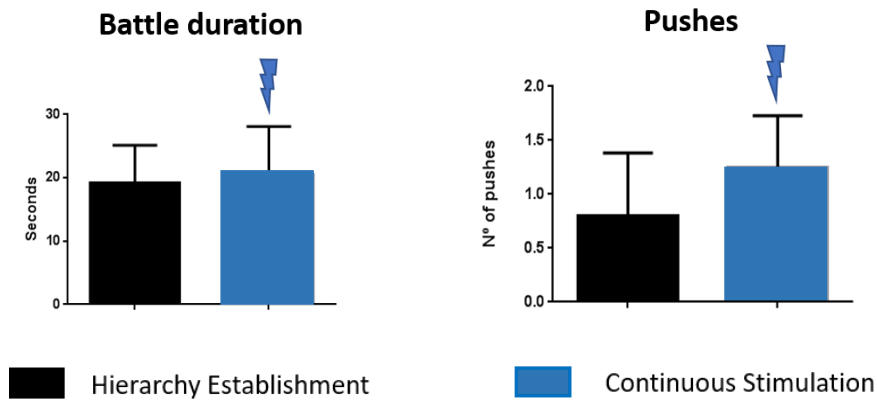
Figure 15: The unilateral and continuous stimulation protocol did not produce significant effects. Figure shows the mean battle duration and mean number of pushes initiated by the stimulated mouse, comparing the battles without stimulation (n=5) and with unilateral stimulation (n=4). Black bars = without stimulation, Grey bars = unilateral stimulation.

Unilateral and continuous stimulation of the lower-ranked individual did not produce significant effect on the animal's behavior, other than a small trend for an increased number of pushes, as shown in **Figure 15**.

We next performed a bilateral stimulation of the targeted animal only after winning a tube test encounter. Additionally, the stimulated mice were selected as middle-ranked, i.e., animals would have both subordinate and dominant opponents. Lastly, after establishing a stable social hierarchy between three animals, we performed two different stimulation protocols: continuous light stimulation and a protocol with modulated light pulses at 100Hz **(Figure 16)**.
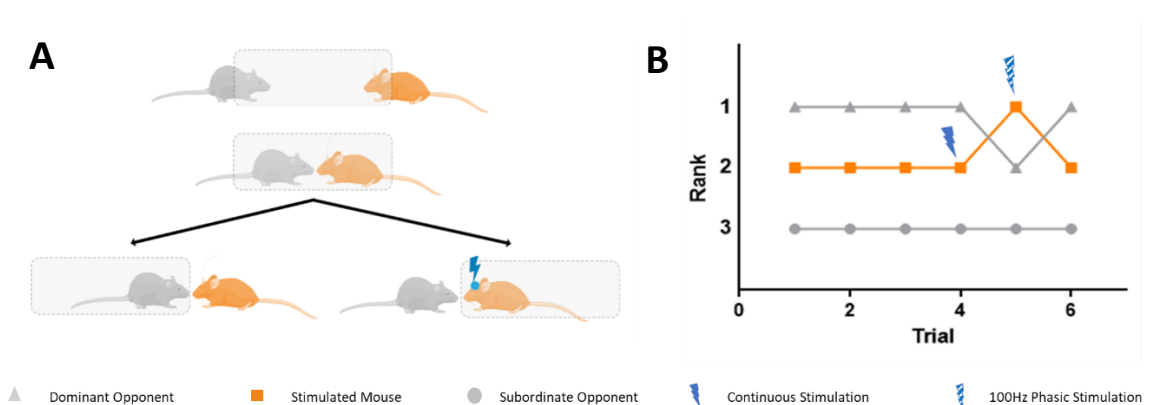
Figure 16: A positive switch in social rank was coincident with the 100Hz light stimulation protocol. A: Stimulation was only applied after a tube test win; **B:** Rank change along 6 trials. Each trial represents a testing day.

After three consecutive days of unaltered hierarchical ranks, the middle-ranked individual was subject to a continuous light protocol for one day (trial 4). The next day (trial 5) a 100Hz phasic light protocol was applied and a positive switch occurred in the social rank between the stimulated mouse and its dominant opponent **(Figure 16, B)**. The rank from the subordinate opponent remained unaltered.

Since two different light protocols were tested, behavior quantification was assessed separately. For each stimulation protocol, quantification was a comparative measure of the behavioral output between trials with and without stimulation ("Hierarchy Establishment"). The behavioral output from the bilateral and continuous light stimulation protocol is shown in **Figure 17**.
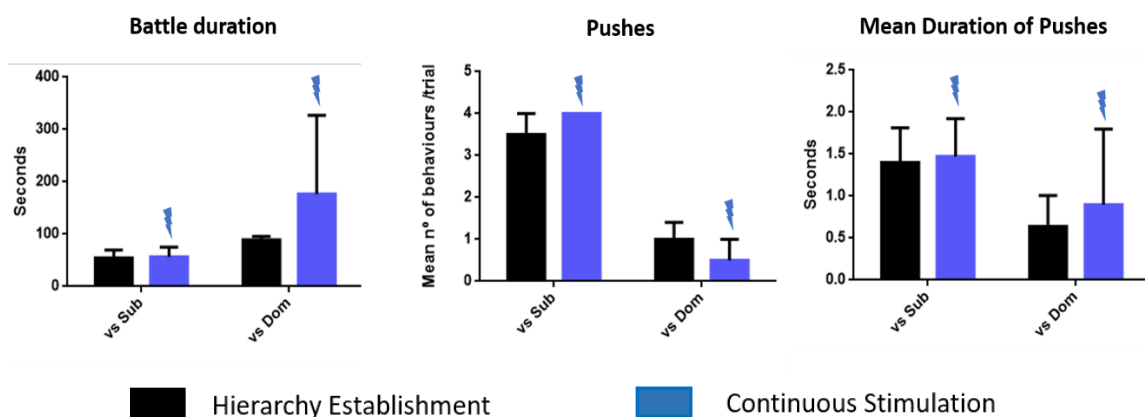
Figure 17: No significant alterations in pushing behaviors were observed with the bilateral and continuous stimulation protocol. The figure shows a comparison for battle duration, number and mean duration of pushes between encounters of the middle-ranked animal against both the dominant and subordinate opponents. Black bars (no stimulation represent an n=4 encounters and grey bars (stimulation) represent an n=2 encounters.

Apart from a tendency to an increased battle duration against the dominant opponent, this stimulation protocol did not appear to influence the stimulated animal's appetence for pushing its opponents **(Figure 17)**.

Additionally, we asked if the stimulation protocol could promote distinctive behaviors towards the dominant opponent, such as resistance periods, that could signal a switch in behavioral pattern towards a more dominant phenotype. Such distinct behaviors were quantified only for encounters between the stimulated mouse and its dominant opponent **(Figure 18)**.
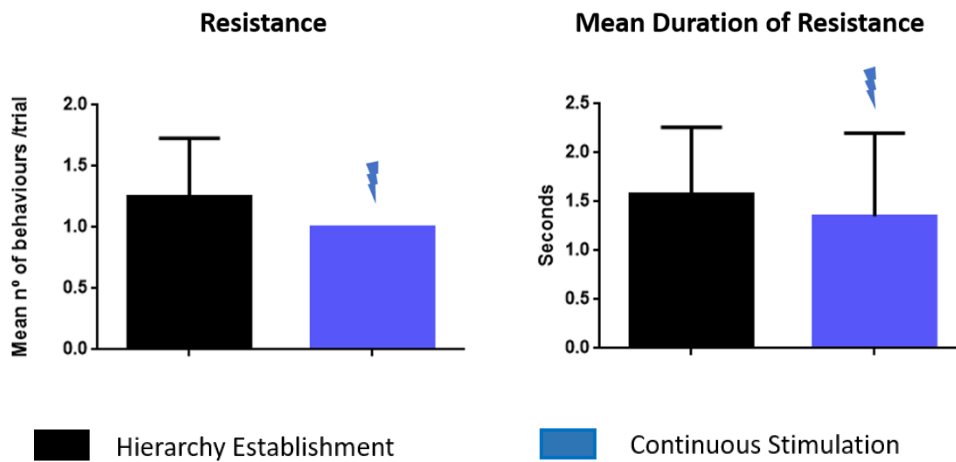
Figure 18: No significant alteration in resistance periods were observed with the bilateral and continuous light stimulation protocol. The figure shows the number and mean duration of resistance behaviors from the middle-ranked animal towards the dominant opponent. Black bars (no stimulation) represent an n=4 encounters and grey bars (stimulation) represent an n=2 encounters.

In addition to unaltered pushing periods, resistance epochs were also not affected by this stimulation protocol. Consequently, we next tested a 100Hz phasic light stimulation protocol **(Figure 19)**.
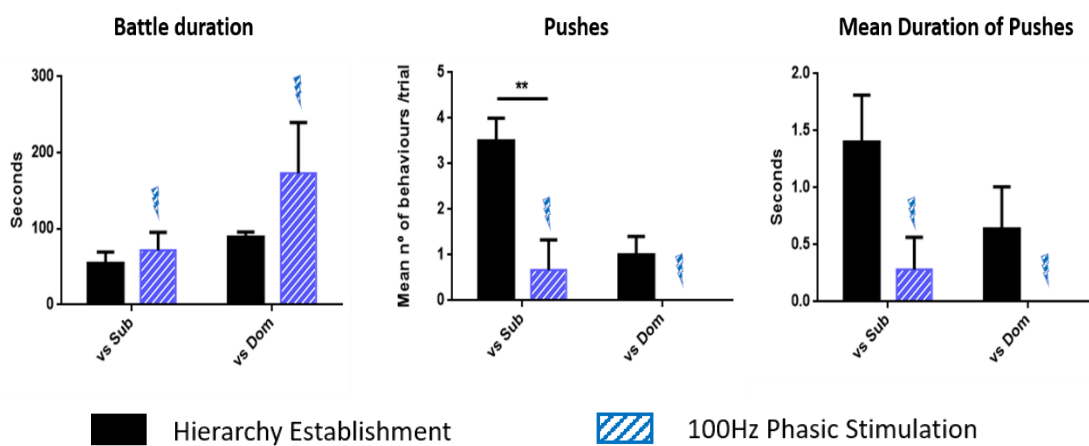
Figure 19: Modulated light stimulation was coincident with a significant decrease in pushing behaviors. The figure shows a comparison for battle duration, number and mean duration of pushes between bouts the middle-ranked animal had against both the dominant and subordinate opponent. Black bars (hierarchy establishment) represent an n=4 bouts and grey bars (100Hz Phasic stimulation) represent an n=3 bouts. The statistical comparisons were performed using Ordinary Two-way ANOVA. Statistical significance was set at *P<0.05, **P<0.01, ***P<0.001. Data are presented as means ±SEM.

The 100Hz phasic stimulation protocol induced a significant decrease in the number of pushes against the subordinate opponent and a tendency towards a decreased mean duration of pushes. Interestingly, no pushes were recorded against the dominant opponent **(Figure 19)**.

Once more, we focused on alterations in distinct behaviors during encounters with the dominant opponent. Despite the absence of pushing behaviors, a switch in hierarchical rank between these two animals was observed. To help clarify this, a more detailed behavioral characterization was performed. Detailed video-decoding helped to decipher the behavioral outcomes of the stimulated mouse **(Figure 20)**.
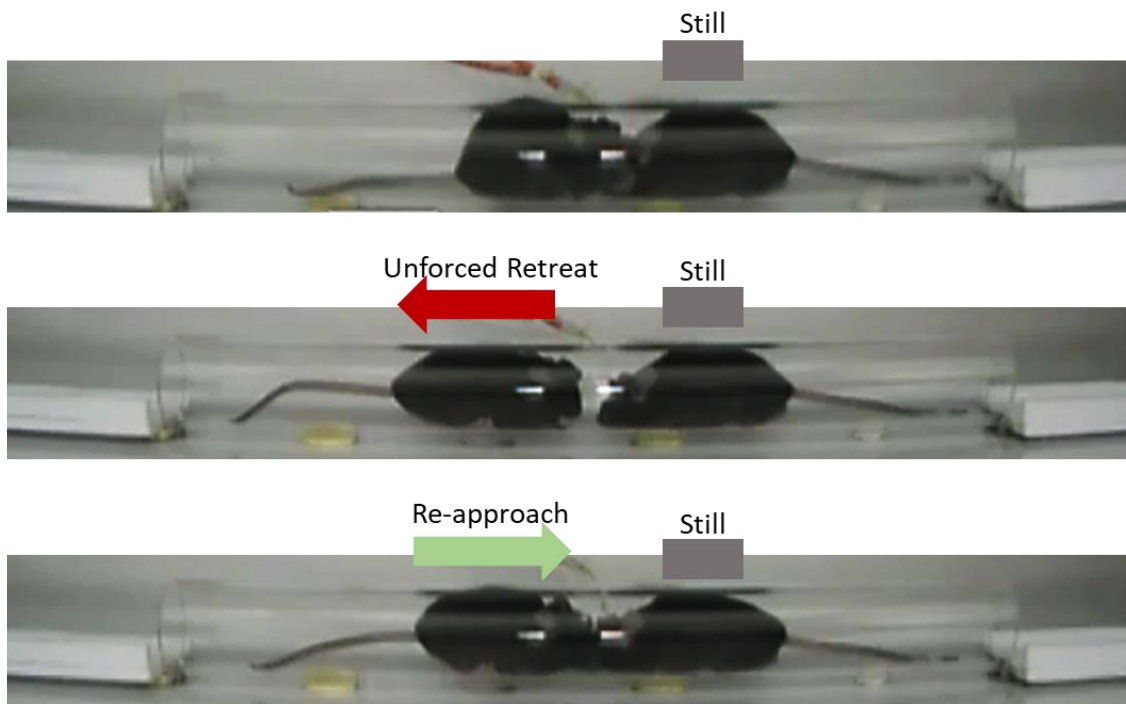
Figure 20: The stimulated animal showed a stereotypical-like behavior during tube test encounters. Video-decoding shows an unforceful retreat by the dominant opponent (left) after engagement with the stimulated mouse (right), followed by a re-approaching at the center of the tube.

Detailed video-decoding shows an increased appetence for the stimulated animal to remain immobile at the center of the tube, not engaging in the dispute with its opponent, during encounters with stimulation. Quantification of such behavior shows a tendency for an increased number and duration of these events **(Figure 21).**

Figure 21: The modulated light stimulation protocol was coincident with an increase in stereotypical-like behaviors. The figure shows a quantification of specific behaviors in encounters between the middle-ranked animal and the dominant opponent. "Opp unsolicited retreats" refers to the number of times the dominant opponent retreated without being forced to and "time spent still" refers to the period of time the middle-ranked animal remained immobile during the encounter. Black bars (no stimulation) represent an n=4 encounters and grey bars (100Hz Phasic stimulation) represent an n=3 bouts. The statistical comparisons were performed using Mann-Whitney U Test. Statistical significance was set at *P<0.05, **P<0.01, ***P<0.001. Data are presented as means ±SEM.

Optimally, a behavioral characterization associated to a positive switch in hierarchical rank would be characterized by increased effortful behaviors, such as the number and mean duration of both pushes and resistance behaviors and/or decrease in retreats[99]. Our results point to a tendency for increase in the number of resistance behaviors. On the other hand, number and mean duration of pushes and resistance periods tend to decrease. This apparent lack of interest from the stimulated animal was manifested negatively in the opponent's behavior. Video-decoding showed how the dominant animal would, at times, retreat without being forced to - i.e., without being pushed by the stimulated animal - a type of behavior that was never observed during encounters without stimulation **(Figures 20 and 21).** Eventually, after repeated unsuccessful tries at pushing the stimulated animal out of the tube, the dominant animal would give up engaging in dispute and exit the tube, consequently being scored as the loser.

Hence, the rank switch between these two animals was not due to increased effortful behaviors from the stimulated mouse but to a seemingly lack of responsiveness that drives the opponent to retreat. The stereotypical behaviors shown here, from both the stimulated animal and its dominant opponent, were not observed during the following testing day, where no stimulation was applied, and the hierarchy reversed back to its original form.

Based on these results, we asked whether the behavioral outcome observed was due to the 100Hz phasic or the continuous stimulation. To tackle this, the experiment was performed again with both light stimulation protocols but extend to a minimum period of two days, while preserving one day between protocols to assess hierarchy ranks **(Figure 22)**. Additionally, for each day of stimulation, an extra round of encounters was performed with the fibers coupled but without stimulation.
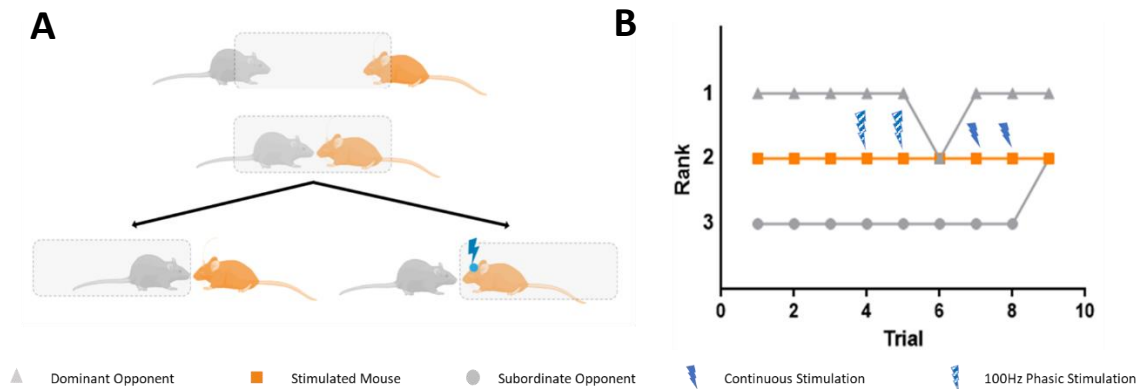
Figure 22: Both stimulation protocols were insufficient to produce a positive switch in hierarchical rank.
A: Stimulation was only applied after a tube test win; **B:** Social ranks change over 9 testing days. Each trial represents a different day of encounters. In trials 4 and 5 a 100Hz phasic light protocol was applied, trial 6 was without stimulation and in trials 7 and 8 was tested a continuous light protocol.

In this experiment, using either of the stimulation protocols, the positive switch in rank previously observed was not replicated. The social rank ties in trials 6 (between stimulated and dominant mice) and 9 (between stimulated and subordinate mice) were a result of an equal number of wins by the pair of mice. Nevertheless, the stimulated animal's hierarchical rank effectively did not change throughout the 9 trials.

The first stimulation protocol, with 100Hz phasic modulated light, was applied for two consecutive days and behavioral characterization represented below **(Figure 23)**.
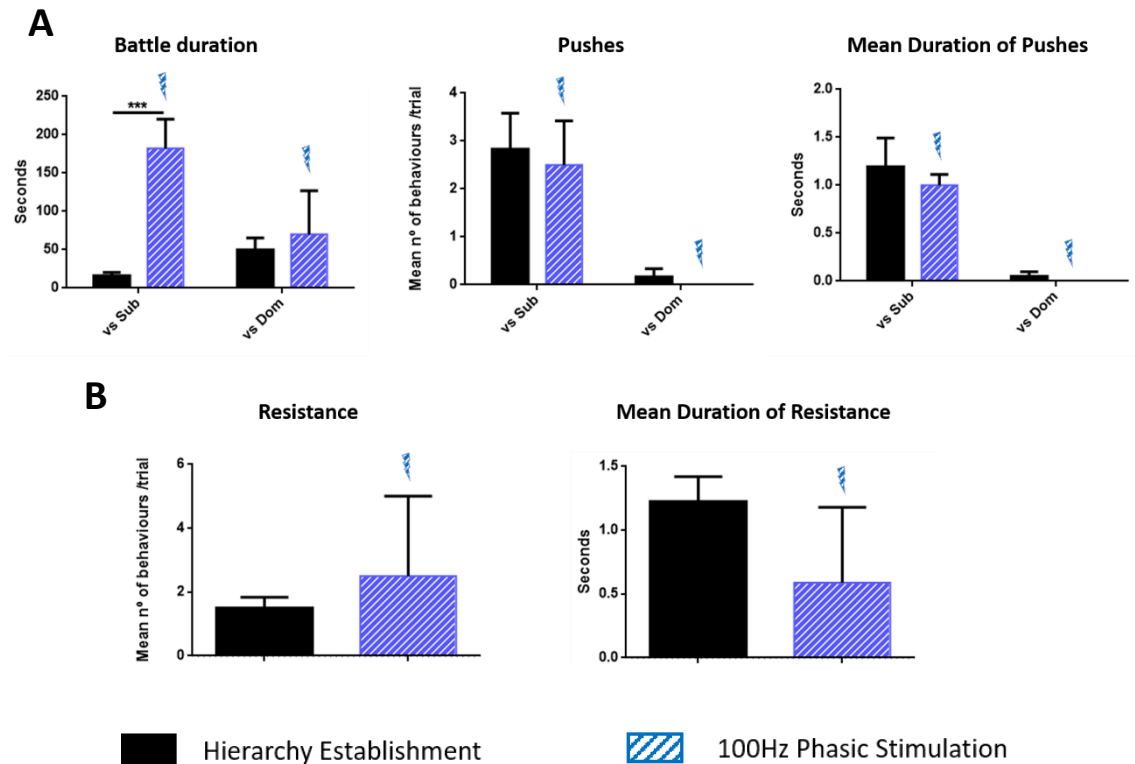
Figure 23: The modulated light protocol produced longer encounters but no significant behavioral alteration. A: Duration, number and mean duration of pushes from the middle-ranked animal against both the dominant and subordinate opponents, for the two days of stimulation protocol. Black bars (no stimulation) represent an n=6 encounters. Grey bars (100Hz Phasic stimulation) represent an n=6 encounters against the subordinate and an n=2 encounters against the dominant opponent. The statistical comparisons were performed using Ordinary Two-way ANOVA. Statistical significance was set at *P<0.05, **P<0.01, ***P<0.001. Data are presented as means ±SEM; **B:** Resistance and mean duration of resistance behaviors of the middle-ranked animal towards the dominant opponent. Black bars (no stimulation) represent an n=6 encounters and grey bars (100Hz Phasic stimulation) represent an n=2 encounters.

The 100Hz phasic light stimulation protocol did not produce a switch in hierarchical rank. Although a significant increase was observed in the duration of the encounters **(Figure 23,A)**, a cessation of pushes in encounters against the dominant opponent was also observed **(Figure 23)**, similarly to previous results **(Figure 19)**.

After a one-day interval, the continuous light stimulation protocol was performed **(Figure 24)**.
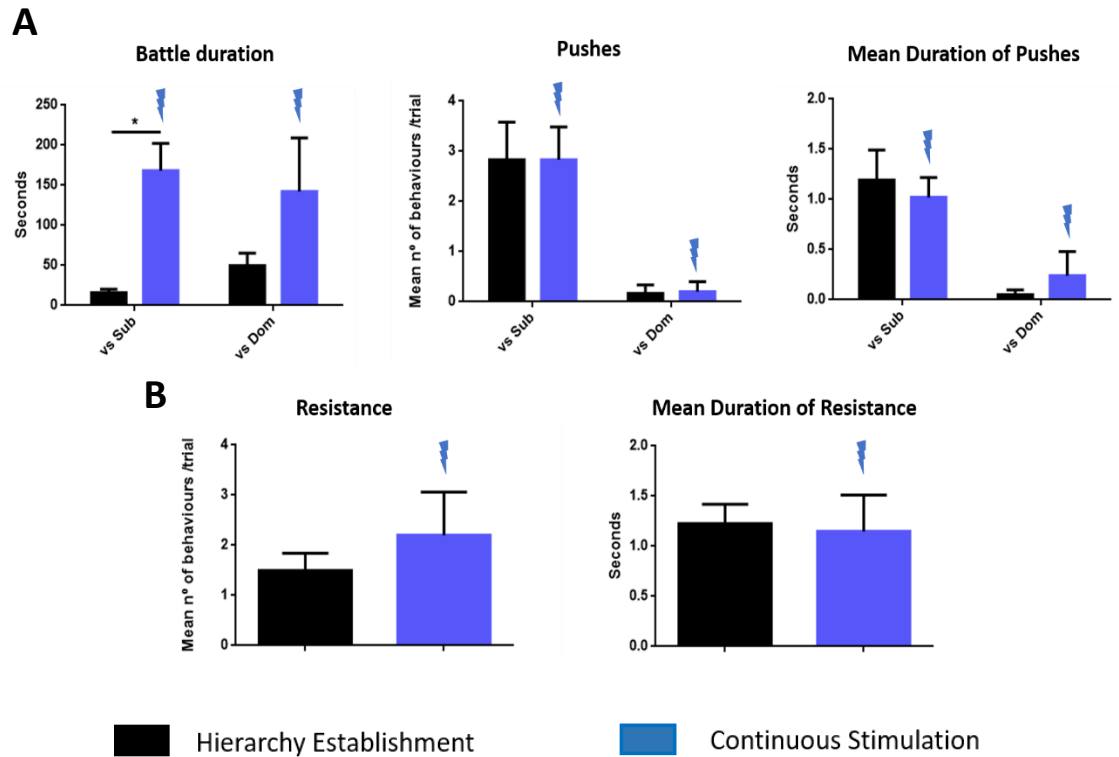
Figure 24: The continuous light protocol produced longer encounters but no significant behavioral alterations A: Battle duration, number and mean duration of pushes of the middle-ranked animal against both the dominant and subordinate opponents. Black bars (no stimulation) represent an n=6 encounters and grey bars (continuous stimulation) represent an n=3 encounters. The statistical comparisons were performed using Ordinary Two-way ANOVA. Statistical significance was set at *P<0.05, **P<0.01, ***P<0.001. Data are presented as means ±SEM; **B:** Resistance and mean duration of resistance behaviors of the middle-ranked animal towards the dominant opponent. Black bars (no stimulation) represent an n=6 encounters and grey bars (continuous stimulation) represent an n=5 encounters.

Hierarchical rank did not alter, although an increased battle duration in stimulated trials was evident **(Figure 24)**. Longer encounters were common to both experiments and did not depend on which light stimulation protocol was applied and whether encounters were against the subordinate or the dominant opponent. Explaining this phenomenon through alterations in effortful behaviors is challenging since stimulated trials seem to only produce small tendencies in the behaviors analyzed.

Since all stimulated trials involve coupling a pair of optic fiber cables to the head of the stimulated animal, we decided to get a measure of how this effect was potentially impacting the coupled animal's behavior and if an increased duration could be a manifestation of tethering the animal. For that, we gathered data on specific behaviors from encounters that involved coupling the fibers but no stimulation and encounters that did not involve coupling the fibers **(Figure 25)**.
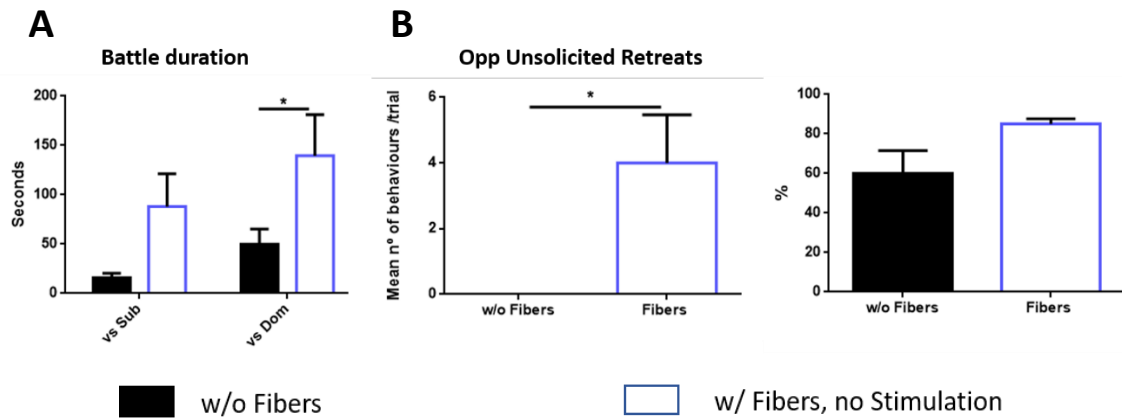
Figure 25: Connection of fibers produced an increase in stereotypical-like behaviors. A: Battle duration between encounters with the middle-ranked animal against both the dominant and subordinate opponent. The statistical comparisons were performed using Ordinary Two-way ANOVA. Statistical significance was set at *P<0.05, **P<0.01, ***P<0.001. Data are presented as means ±SEM; **B:** Quantification of specific behaviors in encounters between the middle-ranked animal and the dominant opponent. "Opp unsolicited retreats" refers to the number of times the dominant opponent retreated without being forced to and "time spent still" refers to the period of time the stimulated animal remained immobile during the encounter. Black bars (w/o Fibers) represent an n=6 encounters and grey bars (with Fibers) represent an n=4 encounters. The statistical comparisons were performed using Mann-Whitney U Test. Statistical significance was set at *P<0.05, **P<0.01, ***P<0.001. Data are presented as means ±SEM.

Similarly to what was observed when a switch in rank was produced during the previous experiment **(Figure 21)**, the coupling of the fibers seemed to produce a stereotypical-like behavior in the stimulated animal, characterized by an increased propensity to stay still in the middle of the tube **(Figure 25)**. This was accompanied by a significant increase in opponents unforceful retreats **(Figure 25)**, as seen before **(Figure 21)**, despite not resulting in a hierarchical rank change. Analyses of the encounters duration also indicate that this phenomenon could be explained by the influence of the fibers **(Figure 25).**

At this point, we asked whether the coupling of the fibers was affecting the animal's motility during encounters. Nevertheless, since the fibers effect was seen only in one animal, the extent of their influence in animal's behavior remained unclear. As such, we designed an experiment that would include days where the fibers were coupled but no stimulation was applied **(Figure 26)**.

A

B

Dominant Opponent ▲   Stimulated Mouse ■   Subordinate Opponent ●   100Hz Phasic Stimulation   Fibers Coupled, no Stimulation
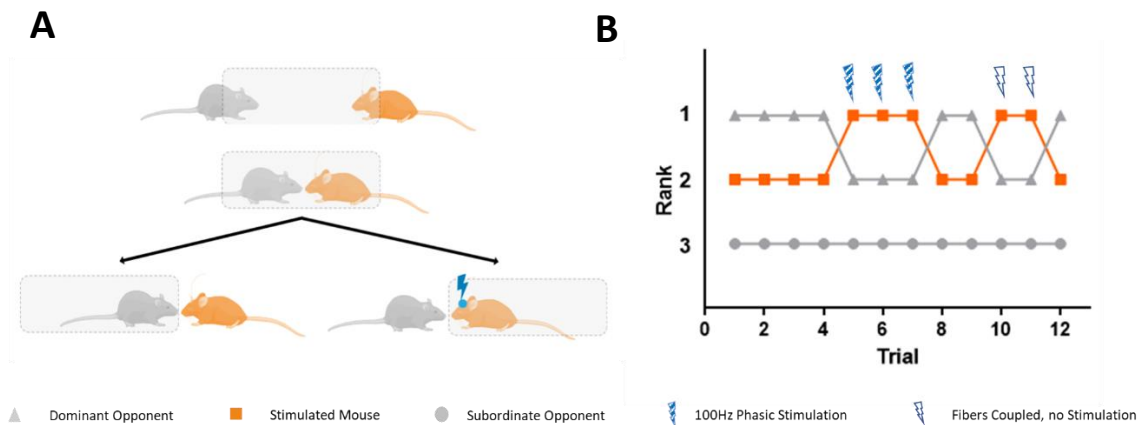
Figure 26: Coupling the fibers to the animal produces an artificial positive switch in hierarchical rank. A: Stimulation was only applied after a tube test win; **B:** Rank change along 12 trials. Each trial represents a day of multiple encounters. In trials 5, 6 and 7 a 100Hz phasic protocol was applied. In trials 10 and 11 the optic fiber cables were coupled to the animal but no stimulation was applied.

This experiment evidenced how coupling the optic fiber cables can produce artificial switches in hierarchical rank **(Figure 26, B)**. Video-decoding of these trials revealed the same stereotypical-type of behaviors seen previously **(Figure 27)**.
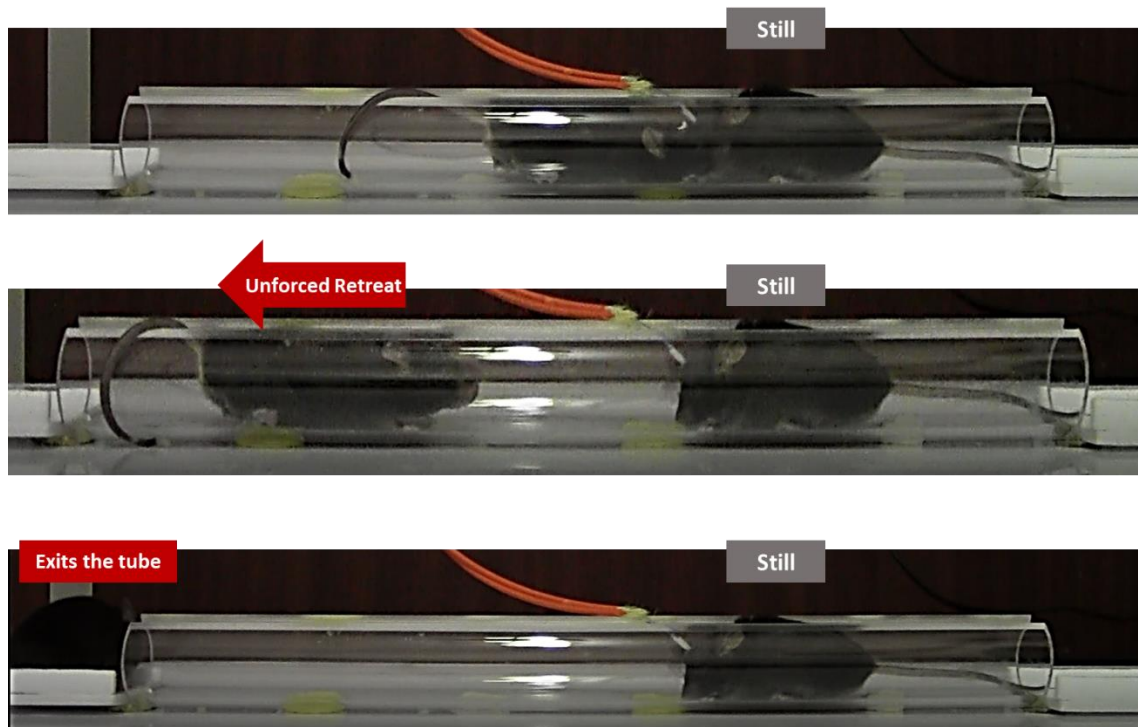
Figure 27: Coupling the fibers to the animal resulted in stereotypical-type behaviors. The figures show a time-lapse of animals' behavior during a trial where the fibers were coupled but no stimulation was applied. The coupled animal (right) remains immobile while its opponent (left) retreats all the way out of the tube, being scored as the loser after 4 seconds.

These evidences suggest that the fibers influence overcomes any effect that the light stimulation protocols may have on the stimulated animal's behavior.

After the behavioral experiments were finished, brains from stimulated mice were imaged and channelrhodopsin expression assessed. Images obtained were compiled to evidence brain regions where expression was observed across all mice **(Figure 28)**.
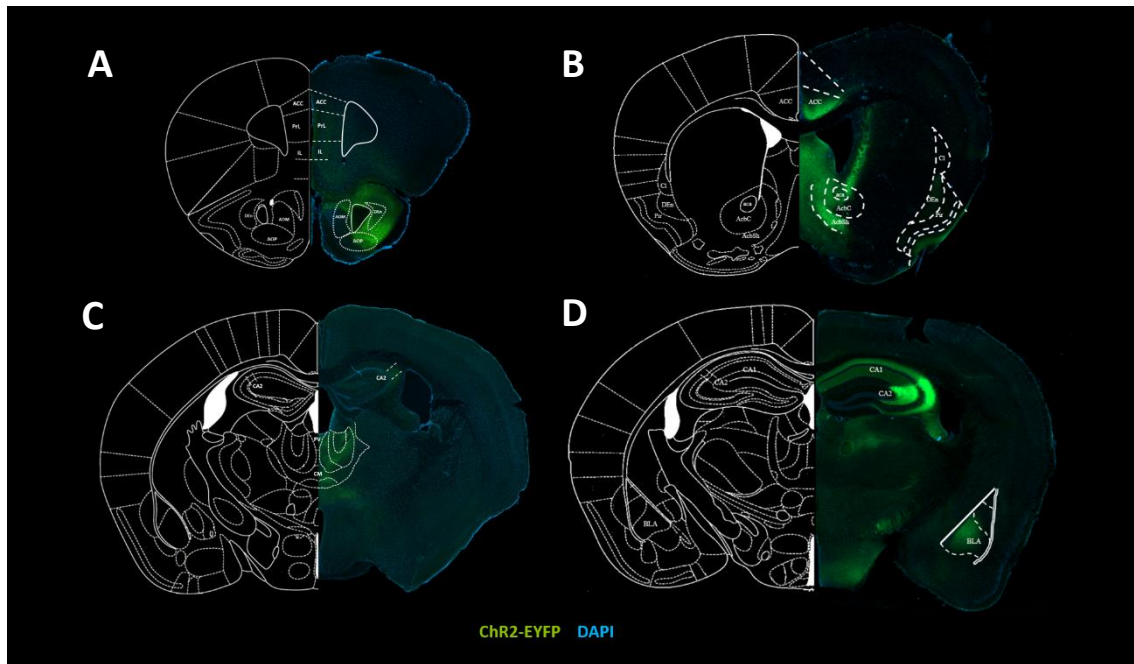
Figure 28: Channelrhodopsin (green) expressed in the NAcc and brain regions known to directly connect to the NAcc. A: Expression is seen along the anterior cingulate, pre-limbic and infra-limbic cortices of the medial pre-frontal cortex and along the anterior olfactory nucleus (Bregma 1.98mm); **B:** Expression is mostly seen along the anterior cingulate, piriform cortex and nucleus accumbens regions (Bregma 0.98mm); **C:** Expression is stronger along the hippocampal CA2 region and in the paraventricular regions of the thalamus (Bregma -1.22mm); **D:** Expression is stronger along the hippocampus - particularly along the CA2 region – and in the basolateral amygdala (Bregma -1.70mm). **Abbreviations:** aca, anterior commissure; AcbC, nucleus accumbens core; AcbSh, nucleus accumbens shell; ACC, anterior cingulate cortex; AOM, anterior olfactory nucleus, medial region; AOP, anterior olfactory nucleus, posterior region; BLA, basolateral amygdala anterior part; CA1, field CA1 of hippocampus; CA2, field CA2 of hippocampus; Cl, claustrum; DEn, dorsal endopiriform nucleus; IL, infra-limbic cortex; Pir, piriform cortex; PrL, pre-limbic cortex; PV, paraventricular thalamic nucleus.

The results show that stimulated mice expressed channelrhodopsin in both NAcc **(Figure 28, B)** and mPFC **(Figure 28, A)**. Similarly to the results obtained after CTB injection, ChR2 also expressed in the paraventricular thalamic nucleus **(Figure 28, C)** and anterior basolateral amygdala **(Figure 28, D)**. Additionally, ChR2 expression was distinctly observed along the anterior olfactory nucleus **(Figure 28, A)**, piriform cortex **(Figure 28, B)** and hippocampus **(Figure 28, C and D)**.

3.4 - Validation of Photo-induced Activation of Neuronal Projections

Immunohistochemistry to label the immediate early gene (IEG) c-Fos was performed to test if the photo-stimulation protocols could induce neuronal activation. For this, a 465nm blue-light, the same as used during stimulation trials, was applied to the mPFC of ChR2-expressing animals. After 90 minutes, the tissue was fixed and c-Fos protein expression was assessed by immunohistochemistry **(Figure 29)**.
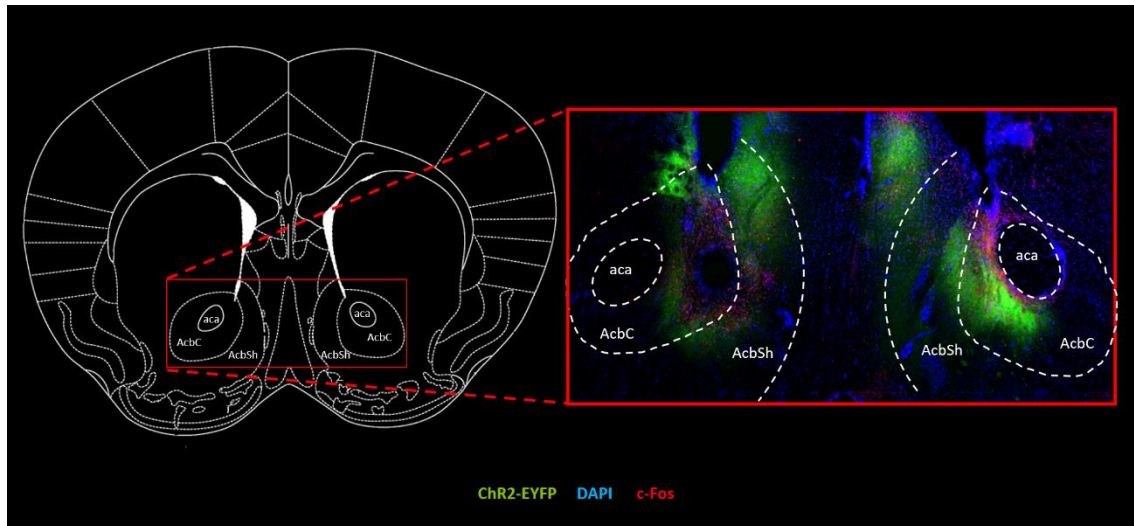
Figure 29: Photo-stimulation of the mPFC results in expression of the immediate early gene c-Fos at the NAcc. The figure shows cells co-expressing ChR2 (green) and c-Fos (red) in the NAcc region (Bregma 1.18mm). **Abbreviations:** aca, anterior commissure; AcbC, nucleus accumbens, core region; AcbSh, nucleus accumbens, shell region.

Here, we show that c-Fos protein labelling is coincident with ChR2 expression **(Figure 29)**. Such co-labelling was particularly strong at the NAcc region,

Chapter 4| Discussion

The mPFC and NAcc regulate important aspects of social dominance behaviors. Nevertheless, it is still necessary to dissect the role the mPFC has in social ranks, including its top-down control over the different downstream nuclei it connects to. The NAcc comes out as an interesting candidate, given its role in reward and effort, which might help to explain how mice wield their effortful behaviors in dominance encounters.

The first goal of this thesis was to anatomically and functionally map the neuronal projections between the mPFC and NAcc regions. To accomplish this, we took advantage of electrophysiology and neuroanatomical tracing techniques. Electrophysiology recordings aim to measure neurons' electrical activity and the mechanistic and cellular proprieties behind them[106]. This can, consequently, help to decipher the role of neurons within a circuit or even at a behavioral level[106]. Neuroanatomical studies, in turn, focus on evidencing wiring patterns between neuronal populations, commonly applied in the identification of cells/neuronal projections that innervate each brain region[107,108]. However, as modern tracers fill the neurons with fluorescent dyes, additional uses can be found, ranging from ultrastructural neuronal analyses to fluorescent cell sorting techniques[109]. Together, these two techniques can provide valuable insight on the topographical, mechanistical and functional proprieties of the neuronal projections of interest.

Regarding electrophysiology recordings, social dominance has been correlated with differential synaptic proprieties of the mPFC[26]. Wang *et al.* (2011) reported that top-ranked individuals display greater amplitude in AMPA-mediated mEPSCs in layer V pyramidal neurons of the mPFC, the primary output neurons of this region[26]. Consequently, we hypothesized that similar differential synaptic proprieties could also manifest in the NAcc, due to a strengthened functional connectivity at the mPFC-NAcc circuit level. To tackle this, we performed sEPSCs and AMPA-mediated mEPSCs recordings in the NAcc of animals with known hierarchical ranks. Our results show that dominant individuals possess increased amplitude of sEPSCs **(Figure 8)** but no differences in AMPA-mediated mEPSCs **(Figure 9).** Spontaneous EPSCs are elicited post-synaptic by an action potential-dependent or via spontaneous release of neurotransmitter in the synapse[110]. As such, variations in these recordings are dependent on intrinsic proprieties of the presynaptic cell/neuronal circuit in study[110,111]. Measures of mEPSCs allow us to clarify the presynaptic contribution to the results obtained. Indeed, changes in mEPSC frequency would point to changes in the presynaptic compartment, such as the probability of neurotransmitter release or the number of neurotransmitter release sites[111]. Our results for mEPSC frequency show that this parameter is unaltered, suggesting that the increased amplitude in sEPSCs observed is rather a result of mPFC-NAcc projection neurons being intrinsically more excitable in dominant mice.

As for the anatomical mapping of mPFC-NAcc projections, such was achieved using the commercially available neuroanatomical tracer cholera toxin B sub-unit (CTB), attached to the green fluorescent dye Alexa Fluor 488. Tracers such as CTB possess several proprieties that make them desirable for anatomical studies. CTB exclusively displays retrograde transport[96], i.e. against the flow of neuronal information. Additionally, it is a monosynaptic tracer, meaning that the resulting labelling is confined to the axons of infected neurons[106]. As so, when CTB is injected

in the NAcc, only neuronal projections to "upstream" brain regions will be evidenced. Furthermore, having the neurons labelled with a fluorescent dye makes them readily visible in a fluorescent microscope. Although we were particularly interested in mapping the anatomical connection between mPFC and NAcc, we have shown every brain region that appeared labelled.

Neurotracer injection at the intended target region, the NAcc, was validated **(Figure 10)**. Successfully targeting the NAcc is a guarantee that the labelling of cells in other brain regions is a direct result of propagated infection from it and not from any other region. Outputs from the mPFC originate from neurons located in the anterior cingulate, pre-limbic and infra-limbic cortices, with the latter being the less labelled structure **(Figure 11)**. Previous studies have also reported that core and shell regions of the NAcc receive corticostriatal projections with distinct origins: the infra-limbic innervates the shell region while pre-limbic and anterior cingulate regions innervate the core region[72,112], following a dorsolateral-to-ventromedial topographical organization **(Figure 4)**. Our results also show distinctive fluorescence signal in the thalamus, below the third ventricle, more precisely in the paraventricular thalamic nucleus **(Figure 12)**. This nucleus is a prominent input of the NAcc[113,114] and was suggested to mediate the expression of opiate-withdrawal-induced physical signs and aversive memory[115]. Indeed, Y. Zhu *et al.* (2016), have reported a similar labelling of this nucleus after CTB injection in the NAcc[115]. Lastly, we reported fluorescent labelling of cells in the anterior basolateral amygdala (BLA) **(Figure 13)**, a brain region well documented to innervate and project to the NAcc[116] and described, for example, to have reward-predictive functions[117]. Importantly, knowledge of the topographical organization of mPFC-NAcc connections was crucial to this work. From the observation that the majority of mPFC neuronal inputs to the NAcc arise from the pre-limbic and anterior cingulate cortices **(Figure 11)**, we have defined the stereotactic surgeries to specifically target and manipulate the activation of these projections, two main goals of this project.

Our results showed that injection of the neuroanatomical tracer CTB in the NAcc resulted in labelled cells in several brain regions that are extensively documented as afferents to the NAcc. However, labelled cells could not be identified in the ventral hippocampus, despite it being a well-known "upstream" connection of this brain region[118,119,120]. We hypothesize that adjustments to the volume/concentration of CTB injected might help improve propagation rates. Additionally, since our data only represents an n=2 brains, further replication of this experiment is required.

For the second main goal of this thesis, we intended to reverse the subordinate behavior of lower-ranked mice into dominant phenotypes and, consequently, promote a positive switch in social rank. As shown previously, mPFC-NAcc neuronal projections in higher-ranked mice are characterized by a higher excitability state. As so, we hypothesized that the stimulation of neuronal activity between mPFC and NAcc regions could induce such switch. To achieve this goal, we resorted to optogenetic techniques, consisting of applying controlled light to light-sensitive neurons[121,122]. Neurons become light-sensitive when induced to express light-gated channels at the surface of their membranes. The most popular light-gated channels have a microbial origin and can be used to either suppress neuronal activity[123,124] or promote it[125]. Our chosen light-gated channel was Channelrhodopsin (ChR2), excitable to blue light (of around

465nm) and conductor of positively charged ions, leading to neuron depolarization and, ultimately, positively modulating neuronal activity[125–127].

In this work, ChR2 channels were stereotactic delivered at the membrane of mPFC-NAcc projection neurons. Such was achieved by injecting adeno-associated viral constructs (AAV's) containing the ChR2 gene to the NAcc. ChR2 expression was not limited to the injection since, and unlike neurotracers such as CTB, AAV's travel both antero and retrogradely (i.e., with and against the flow of neuronal information). As a result, ChR2 also expressed in several other brain regions, including in the mPFC. To stimulate these mPFC-NAcc neurons, we placed an optic fiber ferrule in the mPFC of each brain hemisphere, around the anterior cingulate and pre-limbic cortices, which allowed the delivery of light to this region. This strategy guaranteed that only functional projections from the mPFC to the NAcc were manipulated.

To confirm that these two brain regions were consistently reached, we optimized the stereotactic procedure by rehearsing surgeries **(Supplementary Figure 5)**. A set of coordinates was optimized and later used throughout the rest of the work developed in this thesis based on the "The Mouse Brain in Stereotaxic Coordinates" atlas from George Paxinos[128] and considering that the mouse brain sits inside the skull at a 10° angle[129] **(Supplementary Figure 6)**.

A unilateral and continuous light stimulation protocol during tube test encounters was successfully applied in a previous study to produce instantaneous winning in the tube test, via manipulation of neuronal activity in the mPFC[99]. Zhou *et al.* (2017) have evidenced how stimulated mice would (1) increase their effortful behaviors during tube test encounters, (2) have longer resisting epochs and (3) initiating more pushes[99]. Likewise, we were also interested in promoting a similar behavioral change. More and longer periods of resistance and pushing, and fewer retreats could suggest a more dominant phenotype. And, even if no switch in rank occurred, it was still important to quantify these distinct behaviors. Increased time of resisting pushes from the dominant opponent, for example, might occur and result in prolonged disputes, so tracking the duration of the encounters was also important.

Replicating the stimulation protocol used by Zhou *et al.* (2017) was unfruitful, since no tangible behavior change was observed, even after repeating the protocol for four consecutive days **(Figure 14)**. We hypothesized that unilateral stimulation could be insufficient to recruit a large enough number of projection neurons needed to induce a behavioral alteration. Additionally, we further hypothesized that animal stimulation should be context-dependent and only occur to reinforce an already occurring rewarding stimulus, rather than indiscriminately throughout the behavioral testing.

Based on this hypothesis, we decided to alter the optogenetic paradigm. Bilateral, continuous or phasic (100Hz), protocols were tested but only after a tube test win. The phasic protocol was chosen due to previous studies reporting that dmPFC neurons possess a phasic firing pattern, which 100Hz phasic light efficiently promotes[99,130]. In social hierarchies of at least three individuals, the middle-ranked animal interacts with both dominant and subordinate opponents. As such, the premise of this experiment was to, first, create a dichotic situation, where the middle-ranked animal was stimulated after a win against the subordinate opponent and not stimulated after a loss against the dominant opponent. With this strategy we hypothesized that, as the experience of winning a social encounter is rewarding (and losing is aversive), mice can

be artificially induced into displaying a more effortful and motivated demeanor if a reinforcement of this reward signal was provided. We also hypothesized that, after some time, the middle-ranked animal would seek this reinforced reward signal and eventually start winning tube test encounters against its dominant opponent, effectively provoking a positive switch in hierarchical rank. As so, we could clarify the contribution of the NAcc and mPFC regions not only in dominance behavior and perception but also reward in processing and motivated behaviors.

The first attempt with this new approach resulted in a positive switch in rank - which was coincident with the application of modulated light - and, with it, a strong behavioral output change **(Figures 16 and 20)**. However, it was unclear what produced this behavioral alteration. Because the two different stimulation protocols were applied in consecutive days, it became undistinguishable whether this was an immediate effect of the 100hz phasic light protocol or rather a delayed effect from the continuous light stimulation protocol applied the day before **(Figure 16)**. Not ideally, since the behavior displayed was rather stereotypical, it could also be an effect of animal's impaired motility produced by the coupling of the optic fiber cables **(Figure 20)**. The results obtained in the following experiments suggest that animals indeed respond negatively to the presence of the optic fiber cables, manifested by a decreased motor behavior **(Figures 25 and 27)**. We believe that this was of such impact that, even if either of the applied stimulation protocols (continuous and modulated light) produced an effect on animal's behavior, such information could not be extracted from our results, due to confounding factors. After these experiments we also believed that the fibers were involved in the rank switch seen in **Figure 16**, and not from increased effortful behaviors, as initially intended. Finally, ChR2 expression was assessed in each of the brains of mice that underwent photo-stimulation **(Figure 28)**. Besides the NAcc, these results show that mice expressed ChR2 in common brain regions to the ones observed with CTB, including the mPFC, BLA and paraventricular thalamic nucleus, suggesting propagation originated from the NAcc.

Being able to confirm that the applied photo-stimulation could elicit neuronal firing is a crucial experimental control. Neuronal activation results in the transient transcription of several genes, known as immediate early genes (IEGs)[131]. IEGs, in turn, code for proteins such as cytoskeletal-inter-acting proteins (e.g. Arc) or transcription factors (e.g. Fos)[132]. Here, we have performed immunohistochemistry to label c-Fos as a marker of neuronal activity. Basal levels of c-Fos are usually very low so alterations to its expression are usually attributed to changes in afferent inputs or in external stimuli[133]. Our results show that photo-stimulating the mPFC successfully elicits strong c-Fos expression at the NAcc region **(Figure 29).** Importantly, we have also observed a strong co-expression of ChR2 and c-Fos, which leads us to believe this is in fact a direct result of increased neuronal activity from the stimulation of photo-sensitive mPFC-NAcc neuronal projections.

Chapter 5| Conclusion

In this thesis we found that the mPFC innervates the NAcc with output neurons that originate from the anterior cingulate, pre-limbic and infra-limbic cortices. At a functional level, we gathered data that suggests that these projection neurons naturally possess a more excitable state in higher-ranked individuals, underlying a role of this connection in social dominance. Optogenetic modulation of mPFC-NAcc neuronal activity during tube test encounters would further unveil the importance of these neurons during social dominance behaviors. c-Fos expression results suggest we can photo-induce activation of mPFC-NAcc neurons. However, attempts at applying optogenetic protocols to behaving mice proved unsuccessful, due to technical constraints.

Currently, to strengthen the data collected, additional neuroanatomical, electrophysiology and optogenetic essays are required. Additionally, building on the results presented here, we propose further biochemical and structural characterization of medium spiny neurons of the NAcc, allied with new electrophysiological protocols to validate our findings.

Chapter 6| Supplementary Figures
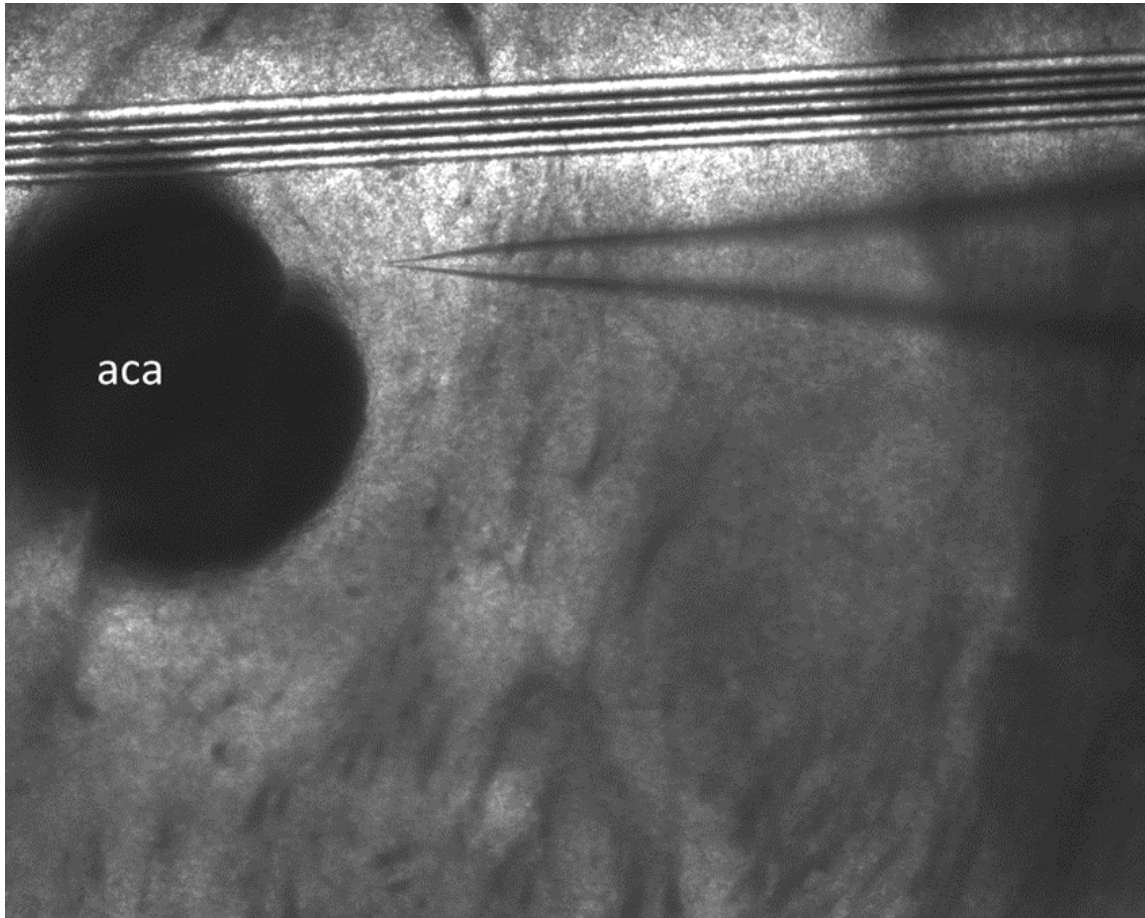
Supplementary figure 1: Patch recordings were performed at the NAcc region. Figure shows a representative image obtained during recordings. **Abbreviations:** aca, anterior commissure.
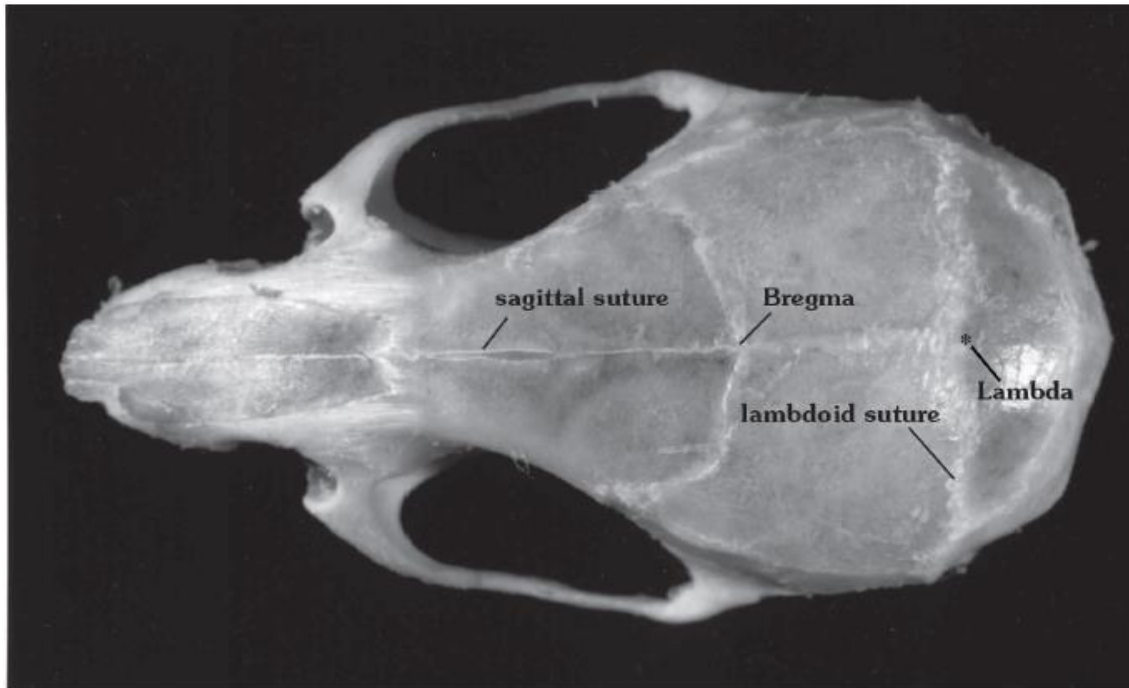
Supplementary figure 2: Bregma and lambda are defined points of intersection along the sagittal and lambdoid sutures. The figure shows a mouse skull diagram showing the horizontal plane reference points bregma and lambda. *Adapted from* Paxinos, G. & Franklin, K. *The Mouse Brain in Stereotaxic Coordinates*. (2013)[128].
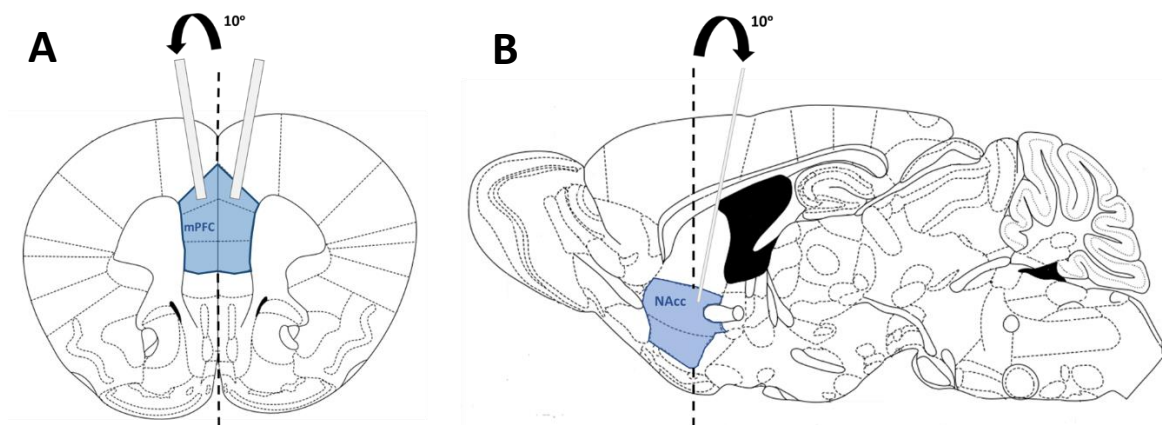
Supplementary figure 3: Schematic figures representing the 10º angles used for viral constructs/neurotracer injection and optic fiber ferrules placement. A: Optic fiber ferrules were inserted into the mPFC with a 10° angle outwards in the medio-lateral axis (Bregma 1.78mm); **B:** Neuroanatomical tracer and AAV-ChR2 constructs were delivered to the NAcc with a glass micropipette at a 10° angle outwards in the rostro-caudal axis (Lateral 0.84mm).
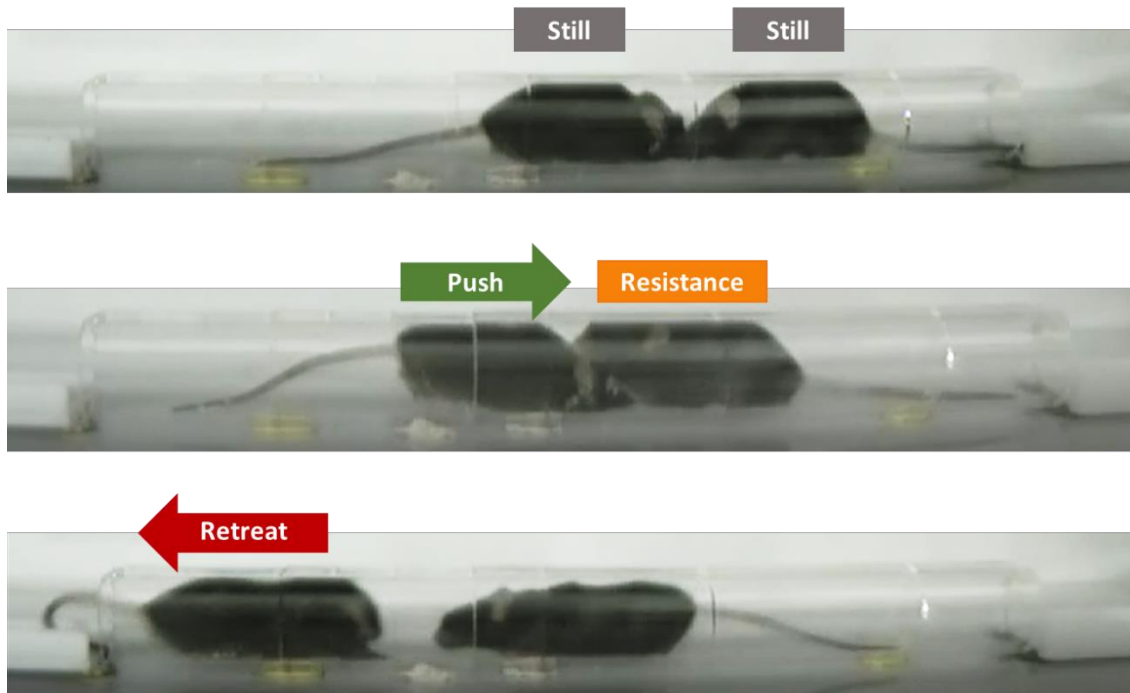
Supplementary figure 4: Characterization of specific behaviors mice display during tube test encounters. Distinct behaviors during tube test encounters were categorized as pushing, stillness, resistance (both when pushing or being pushed) and retreating.

A

B
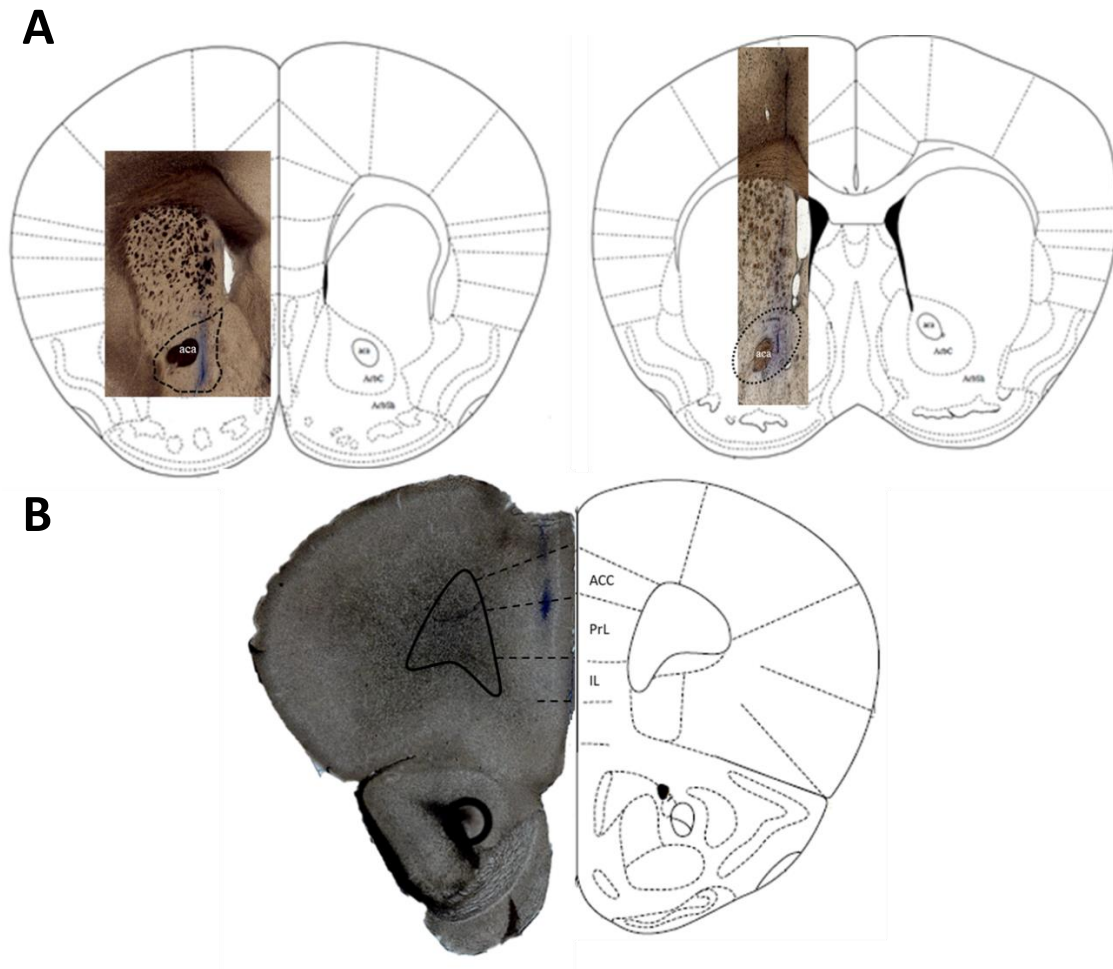
Supplementary figure 5: Successfully reaching the mPFC and NAcc regions during rehearsal surgeries. Figure shows representative images from rehearsal surgeries using an Evans Blue dye (blue). **A:** Targeting the Nucleus Accumbens using the coordinates: 0.8mm medio-lateral axis and 1.5mm on the rostro-caudal axis with a 10º injection angle and final depth of 4mm (Bregma 1.54mm, left and Bregma 1.10mm, right); **B:** Targeting the mPFC using the coordinates 0.6mm medio-lateral axis and 1.8mm on the rostro-caudal axis and final depth of 1.3mm (Bregma 1.98mm). **Abbreviations:** aca, anterior commissure; ACC, anterior cingulate cortex; PrL, pre-limbic cortex; IL, infra-limbic cortex; AcbC, nucleus accumbens, core region; AcbSh, nucleus accumbens, shell region;
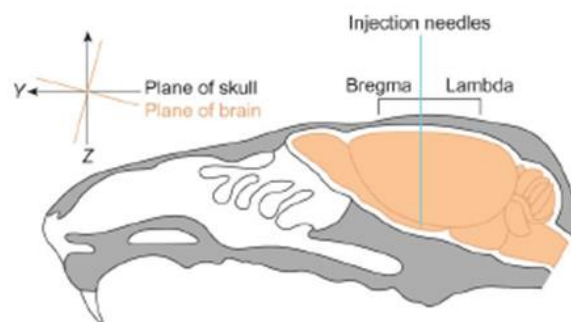
Supplementary figure 6: Relative position of the mouse's brain and skull. *Turning ON Caspases with Genetics and Small Molecules, Charles W. Morgan et al (2014)*[129].

Chapter 7| References

1. Schjelderup-Ebbe, T. Beitrage zur Sozialpsycholgie des Haushuhns. *Zeitschrift Psychol* 225–252 (1922).

2. Dewsbury, D. A. Dominance Rank, Copulatory Behavior, and Differential Reproduction. *Q. Rev. Biol.* (1982). doi:10.1086/412672

3. Kuze, N., Malim, T. P. & Kohshima, S. Developmental changes in the facial morphology of the Borneo orangutan (Pongo pygmaeus): Possible signals in visual communication. *Am. J. Primatol.* (2005). doi:10.1002/ajp.20121

4. Mackinnon, J. The behavior and ecology of wild orangutans (Pongo- Pygmaeus). *Anim. Behav.* 3–74 (1974).

5. Alcazar, R. M., Hilliard, A. T., Becker, L., Bernaba, M. & Fernald, R. D. Brains over brawn : experience overcomes a size disadvantage in fish social hierarchies. 1462–1468 (2014). doi:10.1242/jeb.097527

6. Jarvi, T. On the evolution of inter and intra specific communication through natural and sexual selection. *Ph.D thesis, Univ. Stock.* (1983).

7. Järvi, T. & Bakken, M. The function of the variation in the breast stripe of the great tit (Parus major). *Anim. Behav.* (1984). doi:10.1016/S0003-3472(84)80296-1

8. Wilson, E. O. *Sociobiology, The New Synthesis*.

9. Sapolsky, R. M. 'The Influence of Social Hierarchy on Primate Health': Response. *Science (80-.).* (2005).

10. Halevy, N., Chou, E. Y. & Galinsky, A. D. A functional model of hierarchy: Why, how, and when vertical differentiation enhances group performance. *Organ. Psychol. Rev.* (2011). doi:10.1177/2041386610380991

11. Dalmaso, M., Pavan, G., Castelli, L. & Galfano, G. Social status gates social attention in humans. *Biol. Lett.* (2012). doi:10.1098/rsbl.2011.0881

12. Cheng, J. T., Tracy, J. L., Foulsham, T., Kingstone, A. & Henrich, J. Two ways to the top: Evidence that dominance and prestige are distinct yet viable avenues to social rank and influence. *J. Pers. Soc. Psychol.* (2013). doi:10.1037/a0030398

13. Hymel, S., Closson, L. M., Caravita, S. C. S. & Vaillancourt, T. Social Status Among Peers: From Sociometric Attraction to Peer Acceptance to Perceived Popularity. in *The Wiley-Blackwell Handbook of Childhood Social Development: Second Edition* (2011). doi:10.1002/9781444390933.ch20

14. Zink, C. F. *et al.* Know Your Place: Neural Processing of Social Hierarchy in Humans. **58,** 273–283 (2008).

15. Hall, J. A., Coats, E. J. & LeBeau, L. S. Nonverbal Behavior and the Vertical Dimension of Social Relations: A Meta-Analysis. *Psychol. Bull.* (2005). doi:10.1037/0033-2909.131.6.898

16. Henrich, J. & McElreath, R. The Evolution of Cultural Evolution. *Evolutionary Anthropology* (2003). doi:10.1002/evan.10110

17.   Magee, J. C. & Galinsky, A. D. Social Hierarchy: The Self Reinforcing Nature of Power and Status. *Acad. Manag. Ann.* (2008). doi:10.1080/19416520802211628

18.   Gould, R. V. The Origins of Status Hierarchies: A Formal Theory and Empirical Test. *Am. J. Sociol.* (2002). doi:10.1086/341744

19.   Berry, R. J. Population dynamics of the house mouse. *Symp. Zool. Soc. London* (1981).

20.   Singleton, G. R. & Krebs, C. J. The Secret World of Wild Mice. in *The Mouse in Biomedical Research* (2007). doi:10.1016/B978-012369454-6/50015-7

21.   Lott, D. . Intraspecific Variation in the social systems of wild vertebrates. in *Behavior* (1984).

22.   Van Loo, P. L. P., Mol, J. A., Koolhaas, J. M., Van Zutphen, B. F. M. & Baumans, V. Modulation of aggression in male mice: Influence of group size and cage size. *Physiol. Behav.* (2001). doi:10.1016/S0031-9384(01)00425-5

23.   Hauschka, T. S. Whisker-eating mice. *J. Hered.* (1952).

24.   Nyby, J., Dizinno, G. A. & Whitney, G. Social status and ultrasonic vocalizations of male mice. *Behav. Biol.* (1976). doi:10.1016/S0091-6773(76)92198-2

25.   Whitney, G. & Nyby, J. Cues that elicit ultrasounds from adult male mice. *Integr. Comp. Biol.* (1979). doi:10.1093/icb/19.2.457

26.   Wang, F. *et al.* Bidirectional control of social hierarchy by synaptic efficacy in medial prefrontal cortex. *Science (80-.).* **334,** 693–697 (2011).

27.   Zhou, T. *et al*. History of winning remodels thalamo-PFC circuit to reinforce social dominance. (2017).

28.   LINDZEY, G., WINSTON, H. & MANOSEVITZ, M. Social Dominance in Inbred Mouse Strains. *Nature* **191,** 474–476 (1961).

29.   Wang, F. *et al.* Bidirectional control of social hierarchy by synaptic efficacy in medial prefrontal cortex. *Science* (2011). doi:10.1126/science.1209951

30.   Kalueff, A. V., Minasyan, A., Keisala, T., Shah, Z. H. & Tuohimaa, P. Hair barbering in mice: Implications for neurobehavioural research. *Behav. Processes* (2006). doi:10.1016/j.beproc.2005.09.004

31.   Strozik, E. & Festing, M. F. Whisker trimming in mice. *Lab. Anim.* (1981). doi:10.1258/002367781780953040

32.   de Catanzaro, D. & Ngan, E. T. Dominance in intermale encounters and subsequent sexual success in mice. *J. Comp. Psychol.* (1983). doi:10.1037/0735-7036.97.3.269

33.   Cheney, D. L. . How Monkeys See the World : Inside the Mind of Another Species. 1–2 (1990).

34.   Grosenick, L., Clement, T. S. & Fernald, R. D. Fish can infer social rank by observation alone. **445,** (2007).

35.   Fernald, R. D. Communication about social status. *Current Opinion in Neurobiology* **28,** 1–4 (2014).

36.   Piaget, J. Judgement and Reasoning in the Child. *Harcourt, Brace Company; New York* (1928).

37.   Laidre, M. E. Principles of Animal Communication. *Anim. Behav.* **83,** 865–866 (2012).

38.   Mcintosh, T. K., Barfield, R. J. & Geyer, L. A. Ultrasonic vocalisations facilitate sexual behaviour of female rats. *Nature* **272,** 163–164 (1978).

39.   Wesson, D. W. Sniffing behavior communicates social hierarchy. *Curr. Biol.* **23,** 575–580 (2013).

40.   Chiao, J. Y. *et al.* Knowing Who's Boss: fMRI and ERP Investigations of Social Dominance Perception. *Gr. Process. Intergr. Relations* (2008). doi:10.1177/1368430207088038

41.   Marsh, A. A., Blair, K. S., Jones, M. M., Soliman, N. & Blair, R. J. R. Dominance and Submission: The Ventrolateral Prefrontal Cortex and Responses to Status Cues. *J. Cogn. Neurosci.* (2009). doi:10.1162/jocn.2009.21052

42.   Goldman-Rakic, P. S., Cools, A. R. & Srivastava, K. The Prefrontal Landscape: Implications of Functional Architecture for Understanding Human Mentation and the Central Executive [and Discussion]. *Philos. Trans. R. Soc. B Biol. Sci.* (1996). doi:10.1098/rstb.1996.0129

43.   Mah, L., Arnold, M. C. & Grafman, J. Impairment of social perception associated with lesions of the prefrontal cortex. *Am. J. Psychiatry* (2004). doi:10.1176/appi.ajp.161.7.1247

44.   Prehn, K. *et al.* Individual differences in moral judgment competence influence neural correlates of socio-normative judgments. *Soc. Cogn. Affect. Neurosci.* (2008). doi:10.1093/scan/nsm037

45.   Allison, T., Puce, A. & McCarthy, G. Social perception from visual cues: Role of the STS region. *Trends in Cognitive Sciences* (2000). doi:10.1016/S1364-6613(00)01501-1

46.   Amodio, D. & Frith, C. Meeting of minds: the medial frontal cortex and social cognition. *Nat. Rev. Neurosci.* (2006). doi:10.1038/nrn1884

47.   Lin, A., Adolphs, R. & Rangel, A. Social and monetary reward learning engage overlapping neural substrates. *Soc. Cogn. Affect. Neurosci.* (2012). doi:10.1093/scan/nsr006

48.   Moor, G. B., van Leijenhorst, L., Rombouts, S. a R. B., Crone, E. a & Van der Molen, M. W. Do you like me? Neural correlates of social evaluation and developmental trajectories. *Soc. Neurosci.* (2010). doi:10.1080/17470910903526155

49.   Dawson, G. *et al.* Neurocognitive function and joint attention ability in young children with autism spectrum disorder versus developmental delay. *Child Dev.* (2010).

50.   Gusnard, D. A., Akbudak, E., Shulman, G. L. & Raichle, M. E. Medial prefrontal cortex and self-referential mental activity: relation to a default mode of brain function. *Proc. Natl. Acad. Sci. USA* (2001). doi:10.1073/pnas.071043098

51.   Johnson, S. C. *et al.* Neural correlates of self reflection. *Brain* (2002). doi:10.1093/brain/awf181

52.   Kumaran, D., Banino, A., Blundell, C., Hassabis, D. & Dayan, P. Computations Underlying Social Hierarchy Learning: Distinct Neural Mechanisms for Updating and Representing

Self-Relevant Information. *Neuron* **92,** 1135–1147 (2016).

53. Ligneul, R., Obeso, I., Ruff, C. C. & Dreher, J. C. Dynamical Representation of Dominance Relationships in the Human Rostromedial Prefrontal Cortex. *Curr. Biol.* **26,** 3107–3115 (2016).

54. Karafin, M. S., Tranel, D. & Adolphs, R. Dominance Attributions Following Damage to the Ventromedial Prefrontal Cortex. *J. Cogn. Neurosci.* (2004). doi:10.1162/0898929042947856

55. Blair, R. J. R. Impaired social response reversal: A case of `acquired sociopathy'. *Brain* (2000). doi:10.1093/brain/123.6.1122

56. Rudebeck, P. H. *et al.* Distinct contributions of frontal areas to emotion and social behaviour in the rat. *Eur. J. Neurosci.* (2007). doi:10.1111/j.1460-9568.2007.05844.x

57. Delgado, M. R. Reward-related responses in the human striatum. in *Annals of the New York Academy of Sciences* **1104,** 70–88 (2007).

58. Schultz, W., Apicella, P., Scarnati, E. & Ljungberg, T. Neuronal activity in monkey ventral striatum related to the expectation of reward. *J. Neurosci.* (1992). doi:1432059

59. Tremblay, L., Hollerman, J. R. & Schultz, W. Modifications of reward expectation-related neuronal activity during learning in primate striatum. *J. Neurophysiol.* (1998).

60. Breiter, H. C., Aharon, I., Kahneman, D., Dale, A. & Shizgal, P. Functional imaging of neural responses to expectancy and experience of monetary gains and losses. *Neuron* (2001). doi:10.1016/S0896-6273(01)00303-8

61. Samejima, K. Representation of Action-Specific Reward Values in the Striatum. *Science (80-.).* (2005). doi:10.1126/science.1115270

62. Joshua, M. *et al.* Two types of dopamine neuron distinctly convey positive and negative motivational signals. *Nature* (2011). doi:10.1038/nature08028

63. Fliessbach, K. *et al.* Social comparison affects reward-related brain activity in the human ventral striatum. *Science (80-.).* (2007). doi:10.1126/science.1145876

64. Bault, N., Joffily, M., Rustichini, A. & Coricelli, G. Medial prefrontal cortex and striatum mediate the influence of social comparison on the decision process. *Proc. Natl. Acad. Sci. U. S. A.* (2011). doi:DOI 10.1073/pnas.1100892108

65. Alexander, G. Parallel Organization of Functionally Segregated Circuits Linking Basal Ganglia and Cortex. *Annu. Rev. Neurosci.* (1986). doi:10.1146/annurev.neuro.9.1.357

66. Ferino, F., Thierry, A. M., Saffroy, M. & Glowinski, J. Interhemispheric and subcortical collaterals of medial prefrontal cortical neurons in the rat. *Brain Res.* (1987). doi:10.1016/0006-8993(87)90450-1

67. Wilson, C. J. Morphology and synaptic connections of crossed corticostriatal neurons in the rat. *J. Comp. Neurol.* (1987). doi:10.1002/cne.902630408

68. Lévesque, M., Charara, A., Gagnon, S., Parent, A. & Deschênes, M. Corticostriatal projections from layer V cells in rat are collaterals of long-range corticofugal axons. *Brain Res.* (1996). doi:10.1016/0006-8993(95)01333-4

69.   Gabbott, P. L. A., Warner, T. A., Jays, P. R. L., Salway, P. & Busby, S. J. Prefrontal cortex in the rat: Projections to subcortical autonomic, motor, and limbic centers. *J. Comp. Neurol.* (2005). doi:10.1002/cne.20738

70.   Brog, J. S., Salyapongse, A., Deutch, A. Y. & Zahm, D. S. The patterns of afferent innervation of the core and shell in the ???Accumbens??? part of the rat ventral striatum: Immunohistochemical detection of retrogradely transported fluoro???gold. *J. Comp. Neurol.* (1993). doi:10.1002/cne.903380209

71.   Hauser, T. U., Fiore, V. G., Moutoussis, M. & Dolan, R. J. Computational Psychiatry of ADHD: Neural Gain Impairments across Marrian Levels of Analysis. *Trends Neurosci.* **39,** 63–73 (2016).

72.   Voorn, P., Vanderschuren, L. J. M. J., Groenewegen, H. J., Robbins, T. W. & Pennartz, C. M. A. Putting a spin on the dorsal-ventral divide of the striatum. *Trends Neurosci.* **27,** 468–474 (2004).

73.   Maldonado-Irizarry, C. S. & Kelley, A. E. Differential Behavioral-Effects Following Microinjection of an Nmda Antagonist Into Nucleus-Accumbens Subregions. *Psychopharmacology (Berl).* (1994).

74.   Wu, M., Brudzynski, S. M. & Mogenson, G. J. Functional interaction of dopamine and glutamate in the nucleus accumbens in the regulation of locomotion. *Can. J. Physiol. Pharmacol.* (1993). doi:10.1139/y93-061

75.   Treadway, M. T., Bossaller, N. A., Shelton, R. C. & Zald, D. H. Effort-based decision-making in major depressive disorder: A translational model of motivational anhedonia. *J. Abnorm. Psychol.* **121,** 553–558 (2012).

76.   Salamone, J. D., Correa, M., Nunes, E. J., Randall, P. A. & Pardo, M. The Behavioral Pharmacology of Effort-related Choice Behavior: Dopamine, Adenosine and Beyond. *J. Exp. Anal. Behav.* **97,** 125–146 (2012).

77.   Berridge, K. C. The debate over dopamine's role in reward: The case for incentive salience. *Psychopharmacology* (2007). doi:10.1007/s00213-006-0578-x

78.   Berridge, K. C. & Robinson, T. E. What is the role of dopamine in reward: Hedonic impact, reward learning, or incentive salience? *Brain Research Reviews* (1998). doi:10.1016/S0165-0173(98)00019-8

79.   Saunders, B. T. & Robinson, T. E. The role of dopamine in the accumbens core in the expression of pavlovian-conditioned responses. *Eur. J. Neurosci.* (2012). doi:10.1111/j.1460-9568.2012.08217.x

80.   Chiao, J. Y. Neural basis of social status hierarchy across species. *Current Opinion in Neurobiology* **20,** 803–809 (2010).

81.   Lindner, M., Hundhammer, T., Ciaramidaro, A., Linden, D. E. J. & Mussweiler, T. The neural substrates of person comparison-An fMRI study. *Neuroimage* **40,** 963–971 (2008).

82.   Farrow, T. F. D. *et al.* Higher or lower? The functional anatomy of perceived allocentric social hierarchies. *Neuroimage* **57,** 1552–1560 (2011).

83.   Todorov, A. & Engell, A. D. The role of the amygdala in implicit evaluation of emotionally neutral faces. *Soc. Cogn. Affect. Neurosci.* **3,** 303–312 (2008).

84. Chiao, J. Y. *et al.* Neural representations of social status hierarchy in human inferior parietal cortex. *Neuropsychologia* **47,** 354–363 (2009).

85. Mason, M., Magee, J. C. & Fiske, S. T. Neural Substrates of Social Status Inference: Roles of Medial Prefrontal Cortex and Superior Temporal Sulcus. *J. Cogn. Neurosci.* **26,** 1131–1140 (2014).

86. Marsh, A. A., Blair, K. S., Jones, M. M., Soliman, N. & Blair, R. J. R. Dominance and Submission: The Ventrolateral Prefrontal Cortex and Responses to Status Cues. *J. Cogn. Neurosci.* **21,** 713–724 (2009).

87. Zink, C. F. *et al.* Know Your Place: Neural Processing of Social Hierarchy in Humans. *Neuron* **58,** 273–283 (2008).

88. Dunne, S. & O'Doherty, J. P. Insights from the application of computational neuroimaging to social neuroscience. *Current Opinion in Neurobiology* **23,** 387–392 (2013).

89. Behrens, T. E. J., Hunt, L. T. & Rushworth, M. F. S. The computation of social behavior. *Science* **324,** 1160–1164 (2009).

90. Qu, C., Ligneul, R., Van der Henst, J. B. & Dreher, J. C. An Integrative Interdisciplinary Perspective on Social Dominance Hierarchies. *Trends Cogn. Sci.* **21,** 893–908 (2017).

91. Bartels, A. & Zeki, S. The neural basis of romantic love. *Neuroreport* (2000).

92. Young, L. J., Lim, M. M., Gingrich, B. & Insel, T. R. Cellular mechanisms of social attachment. *Horm. Behav.* (2001). doi:10.1006/hbeh.2001.1691

93. Aragona, B. J. *et al.* Nucleus accumbens dopamine differentially mediates the formation and maintenance of monogamous pair bonds. *Nat. Neurosci.* (2006). doi:10.1038/nn1613

94. Amadei, E. A. *et al.* Dynamic corticostriatal activity biases social bonding in monogamous female prairie voles. *Nature* (2017). doi:10.1038/nature22381

95. Peça, J., Ting, J. T., Wang, W., Wells, M. F. & Venkatraman, T. N. Shank3 mutant mice display autistic-like behaviours and striatal dysfunction. 1–10 (2011). doi:10.1038/nature09965

96. Conte, W. L., Kamishina, H. & Reep, R. L. Multiple neuroanatomical tract-tracing using fluorescent Alexa Fluor conjugates of cholera toxin subunit B in rats. *Nat. Protoc.* **4,** 1157–1166 (2009).

97. Sparta, D. R. *et al.* Construction of implantable optical fibers for long-term optogenetic manipulation of neural circuits. *Nat. Protoc.* **7,** 12–23 (2012).

98. Osten, P., Cetin, A., Komai, S., Eliava, M. & Seeburg, P. H. Stereotaxic gene delivery in the rodent brain. *Nat. Protoc.* **1,** 3166–3173 (2007).

99. Zhou, T. *et al.* History of winning remodels thalamo-PFC circuit to reinforce social dominance. *Science (80-.).* **357,** 162–168 (2017).

100. Courtiol, E. & Wilson, D. A. Thalamic olfaction: characterizing odor processing in the mediodorsal thalamus of the rat. *J. Neurophysiol.* **111,** 1274–1285 (2014).

101. Zitnik, G. A., Clark, B. D. & Waterhouse, B. D. Effects of intracerebroventricular

corticotropin releasing factor on sensory-evoked responses in the rat visual thalamus. *Brain Res.* **1561,** 35–47 (2014).

102. Bartlett, E. L. The organization and physiology of the auditory thalamus and its role in processing acoustic features important for speech perception. *Brain and language* **126,** 29–48 (2013).

103. Castro-Alamancos, M. A. Different temporal processing of sensory inputs in the rat thalamus during quiescent and information processing states in vivo. *J. Physiol.* **539,** 567–578 (2002).

104. Hermans, E. J. *et al.* How the amygdala affects emotional memory by altering brain network properties. *Neurobiology of Learning and Memory* **112,** 2–16 (2014).

105. Wang, S. *et al.* Neurons in the human amygdala selective for perceived emotion. *Proc. Natl. Acad. Sci.* **111,** E3110–E3119 (2014).

106. Lanciego, J. L. & Wouterlood, F. G. A half century of experimental neuroanatomical tracing. *J. Chem. Neuroanat.* **42,** 157–183 (2011).

107. Park, M. Combined social and spatial coding in a descending projection from the prefrontal cortex. (2017).

108. Franklin, T. B. *et al.* Prefrontal cortical control of a brainstem social behavior circuit. *Nat. Neurosci.* **20,** 260–270 (2017).

109. Köbbert, C. *et al.* Current concepts in neuroanatomical tracing. *Prog. Neurobiol.* **62,** 327–351 (2000).

110. Pinheiro, P. S. & Mulle, C. Presynaptic glutamate receptors: physiological functions and mechanisms of action. *Nat. Rev. Neurosci.* **9,** 423–436 (2008).

111. Walz, W. *Electrophysiological Analysis of Synaptic Transmission Series Editor*.

112. Berendse, H. W., Graaf, Y. G. & Groenewegen, H. J. Topographical organization and relationship with ventral striatal compartments of prefrontal corticostriatal projections in the rat. *J. Comp. Neurol.* **316,** 314–347 (1992).

113. Hsu, D. T. & Price, J. L. Paraventricular thalamic nucleus: Subcortical connections and innervation by serotonin, orexin, and corticotropin-releasing hormone in Macaque monkeys. *J. Comp. Neurol.* **512,** 825–848 (2009).

114. Hsu, D. T., Kirouac, G. J., Zubieta, J.-K. & Bhatnagar, S. Contributions of the paraventricular thalamic nucleus in the regulation of stress, motivation, and mood. *Front. Behav. Neurosci.* **8,** 1–10 (2014).

115. Zhu, Y., Wienecke, C. F. R., Nachtrab, G. & Chen, X. A thalamic input to the nucleus accumbens mediates opiate dependence. **530,** 219–222 (2016).

116. Beyeler, A. *et al.* Organization of Valence-Encoding and Projection-Defined Neurons in the Basolateral Amygdala. *Cell Rep.* **22,** 905–918 (2018).

117. Beyeler, A. *et al.* Divergent Routing of Positive and Negative Information from the Amygdala during Memory Retrieval. *Neuron* **90,** 348–361 (2016).

118. Britt, J. P. *et al.* Synaptic and Behavioral Profile of Multiple Glutamatergic Inputs to the

Nucleus Accumbens. *Neuron* **76,** 790–803 (2012).

119. Friedman, D. P., Aggleton, J. P. & Saunders, R. C. Comparison of hippocampal, amygdala, and perirhinal projections to the nucleus accumbens: Combined anterograde and retrograde tracing study in the macaque brain. *J. Comp. Neurol.* **450,** 345–365 (2002).

120. O'Donnell, P. & Grace, A. a. Synaptic interactions among excitatory afferents to nucleus accumbens neurons: hippocampal gating of prefrontal cortical input. *J. Neurosci.* **15,** 3622–3639 (1995).

121. Fenno, L., Yizhar, O. & Deisseroth, K. The Development and Application of Optogenetics. *Annu. Rev. Neurosci.* **34,** 389–412 (2011).

122. Sciamanna, G., Ponterio, G., Mandolesi, G., Bonsi, P. & Pisani, A. Optogenetic stimulation reveals distinct modulatory properties of thalamostriatal vs corticostriatal glutamatergic inputs to fast-spiking interneurons. *Sci. Rep.* **5,** 16742 (2015).

123. Schobert, B. & Lanyi, J. K. Halorhodopsin is a light-driven chloride pump. *J. Biol. Chem.* (1982). doi:10.1146/annurev.biophys.15.1.11

124. Zhao, S. *et al.* Improved expression of halorhodopsin for light-induced silencing of neuronal activity. *Brain Cell Biol.* (2008). doi:10.1007/s11068-008-9034-7

125. Nagel, G. *et al.* Channelrhodopsin-2, a directly light-gated cation-selective membrane channel. *Proc. Natl. Acad. Sci.* (2003). doi:10.1073/pnas.1936192100

126. Arenkiel, B. R. *et al.* In Vivo Light-Induced Activation of Neural Circuitry in Transgenic Mice Expressing Channelrhodopsin-2. (2007). doi:10.1016/j.neuron.2007.03.005.In

127. Ada C. Felix-Ortiz, Anthony Burgos-Robles, Neha D. Bhagat, Christopher A. Leppla, and K. M. T. Bidirectional modulation of anxiety-related and social behaviors by amygdala projections to the medial prefrontal cortex. *Neuroscience* (2016). doi:10.1002/nbm.3369.Three

128. Paxinos, G. & Franklin, K. *The Mouse Brain in Stereotaxic Coordinates*. (2013).

129. Morgan, C. W., Julien, O., Unger, E. K., Shah, N. M. & Wells, J. A. Turning on caspases with genetics and small molecules. *Methods Enzymol.* **544,** 179–213 (2014).

130. Yang, C. R. & Seamans, J. K. Dopamine D1 receptor actions in layers V-VI rat prefrontal cortex neurons in vitro: modulation of dendritic-somatic signal integration. *J Neurosci* **16,** 1922–1935 (1996).

131. Hoffman, G. E., Smith, M. S. & Verbalis, J. G. c-Fos and related immediate early gene products as markers of activity in neuroendocrine systems. *Frontiers in Neuroendocrinology* **14,** 173–213 (1993).

132. Kovács, K. J. Measurement of immediate-early gene activation- c-fos and beyond. *J. Neuroendocrinol.* **20,** 665–672 (2008).

133. Luckman, S. M., Dyball, R. E. & Leng, G. Induction of c-fos expression in hypothalamic magnocellular neurons requires synaptic activation and not simply increased spike activity. *J. Neurosci.* **14,** 4825–4830 (1994).